
Characterisation of HFS Detectors

Sofía Otero Ugobono^{1,2}

*A. Bhardwaj³, R. Dalal³, M. Gallinaro⁴, J. B. González Jiménez^{1,5}, B. Harrop⁶, G. Jain³, C. Lu⁶,
I. Mateu Suau^{1,5}, M. McClish⁷, K. McDonald⁶, M. Moll¹, K. Ranjan³, S. White¹*

¹CERN

²Universidade de Santiago de Compostela

³University of Delhi

⁴LIP

⁵Centro de Investigaciones Energéticas Medioambientales y Tecnológicas

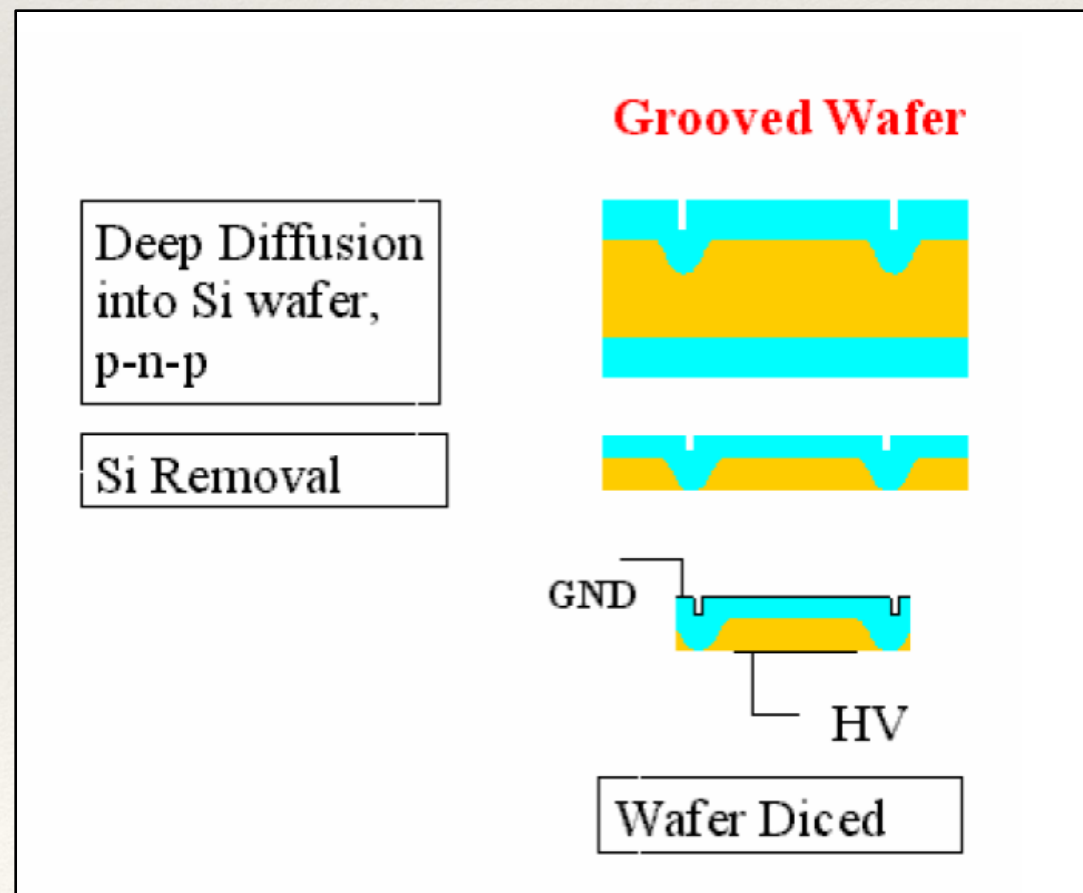
⁶Princeton University

⁷RMD

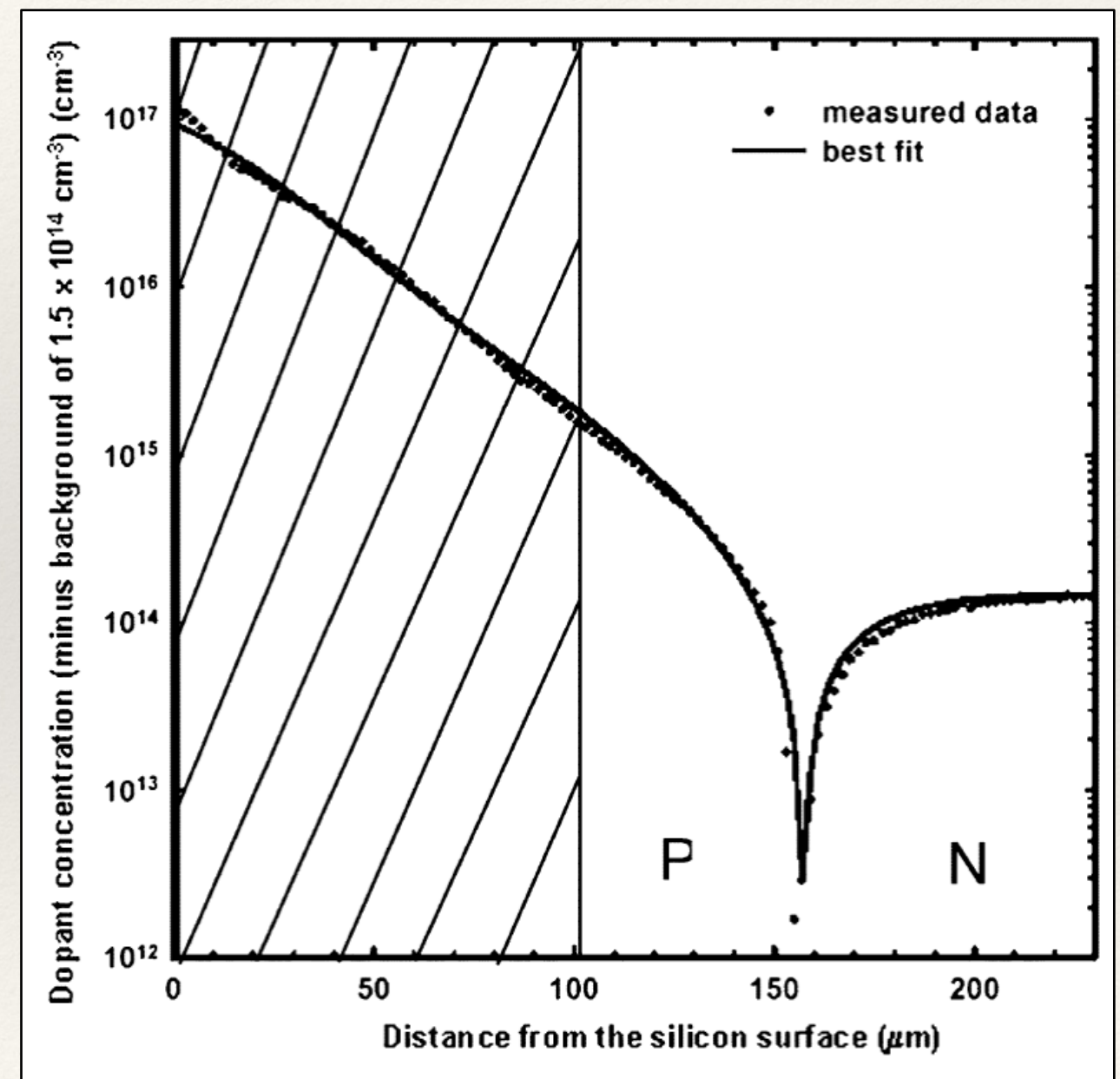
Hyper Fast Silicon Detectors

- ❖ Manufactured by RMD (Radiation Monitoring Devices Inc.)
- ❖ **Based on Deep Diffused APD**
 - ❖ n-type NTD-doped silicon from Topsil
 - ❖ Grooving wafer
 - ❖ Deep diffusion of p-type dopants
 - ❖ Gallium used as dopant
 - ❖ Etching of surface layer

[2006, McClish et al., IEEE TNS, 53, 3049]



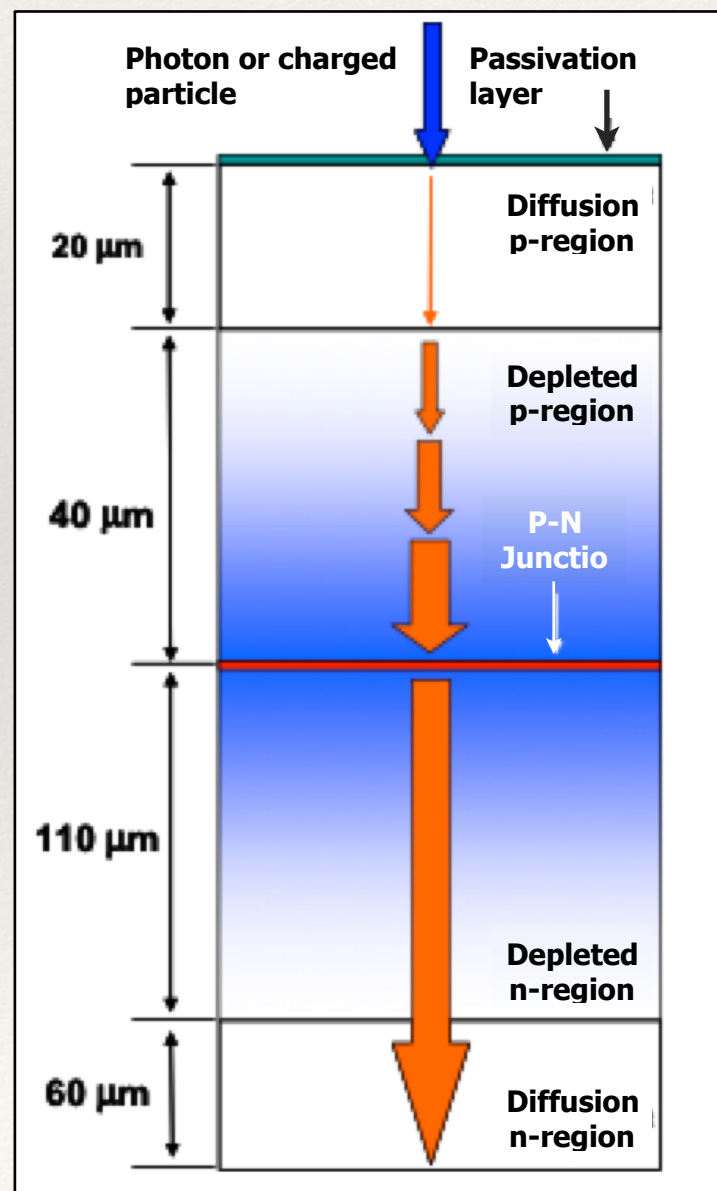
[2004, McClish et al., IEEE TNS]



Charge Multiplication and Gain

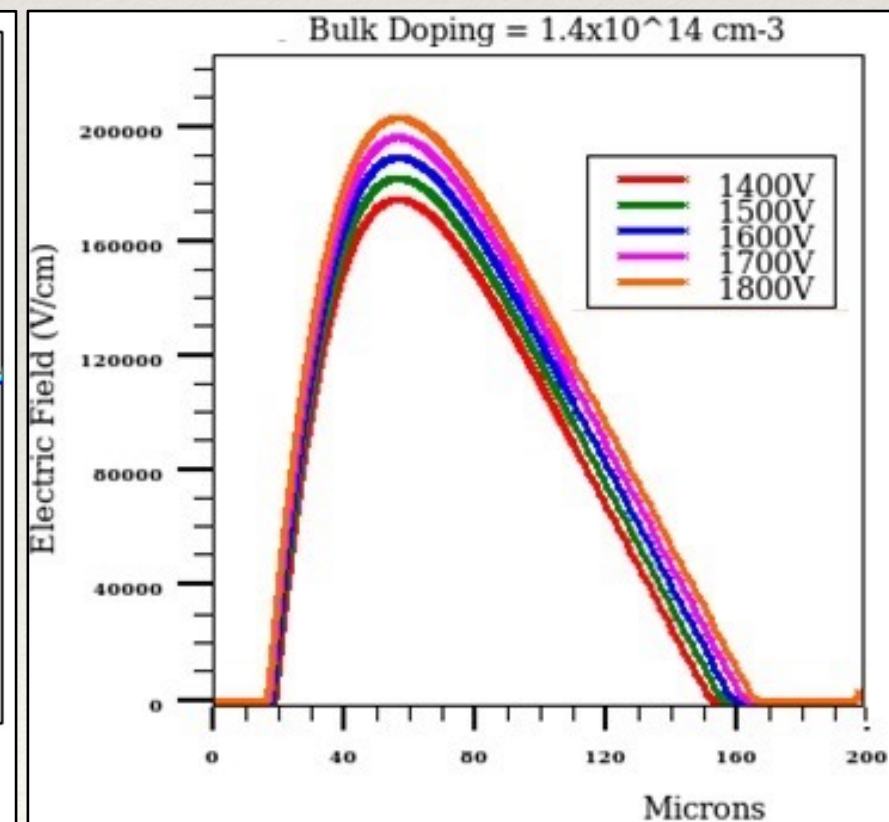
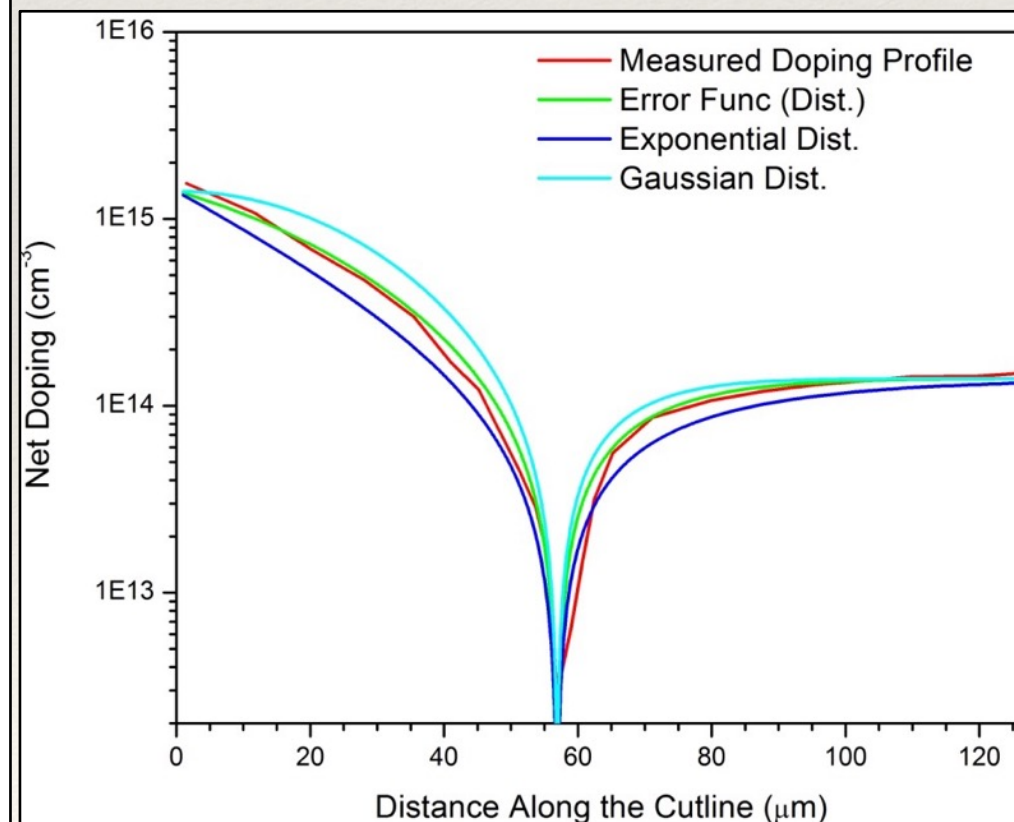
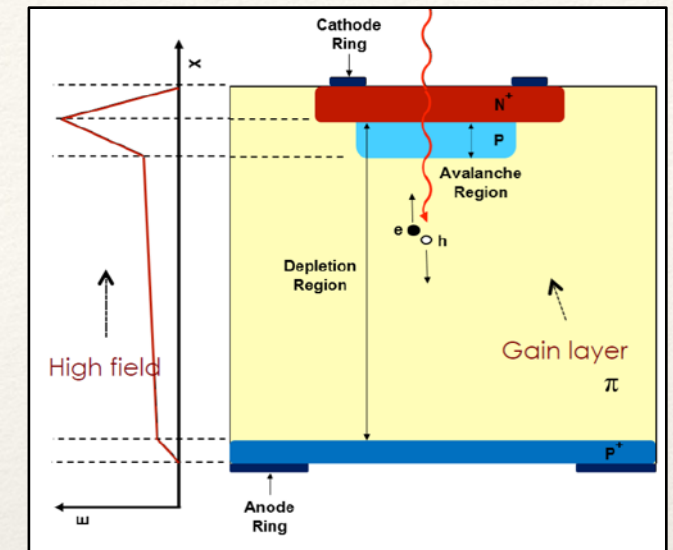
❖ Deep Diffused APDs

- ❖ Amplification deep inside the bulk of the sensor
- ❖ Requires high voltage (1700 V - 1800 V)
- ❖ Delivers high gain and fast response time



❖ TCAD Simulations

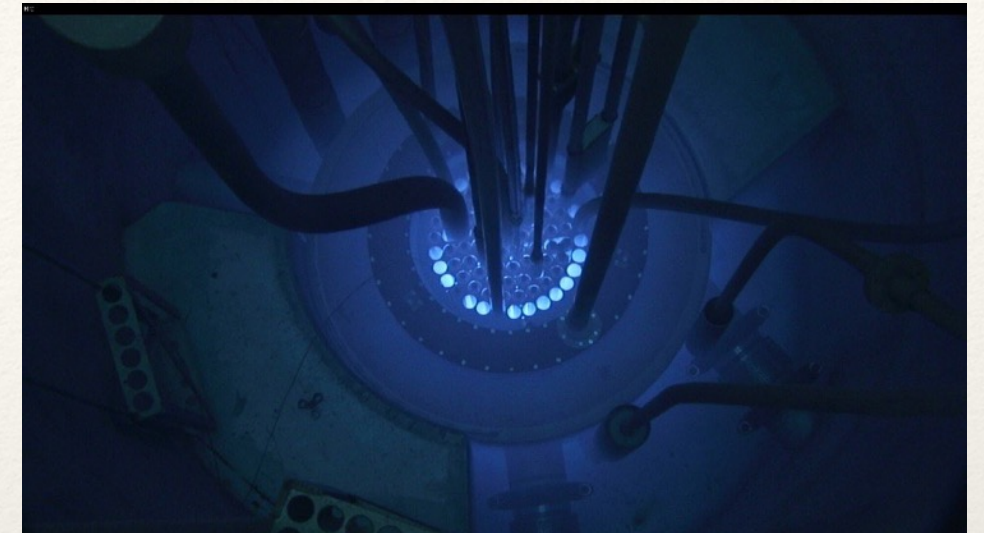
- ❖ Doping profile based on measured data (literature) used to simulate the E-field.



Samples and Measurements

7 HFS detectors

- ❖ 2 left for reference (unirradiated)
- ❖ 5 sent to Ljubljana for neutron irradiation
 - ❖ $3\text{E}13 \text{ n/cm}^2$
 - ❖ $6\text{E}13 \text{ n/cm}^2$
 - ❖ $3\text{E}14 \text{ n/cm}^2$
(two samples received this fluence)
 - ❖ $1\text{E}15 \text{ n/cm}^2$



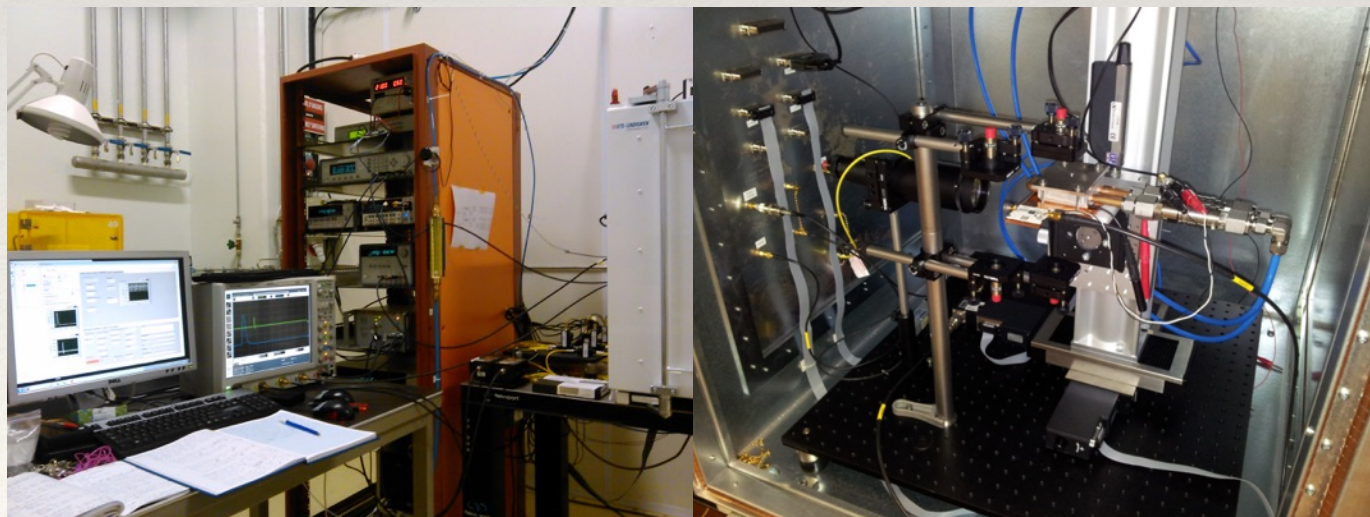
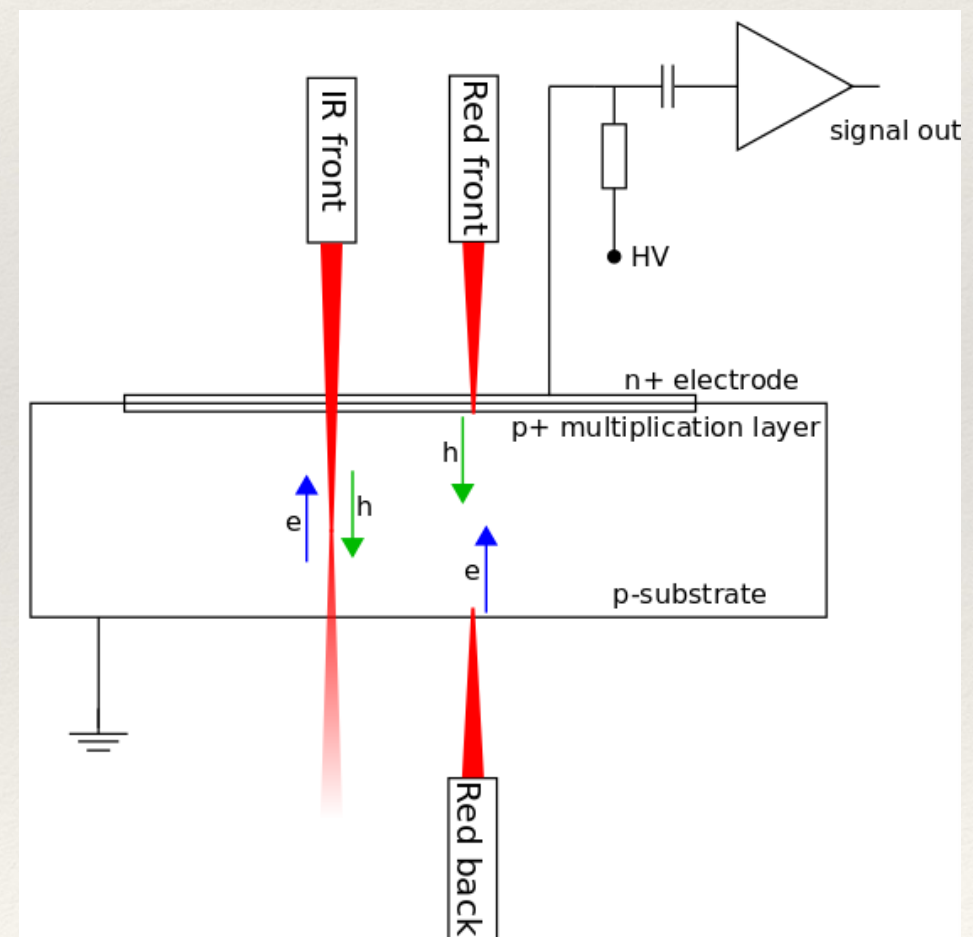
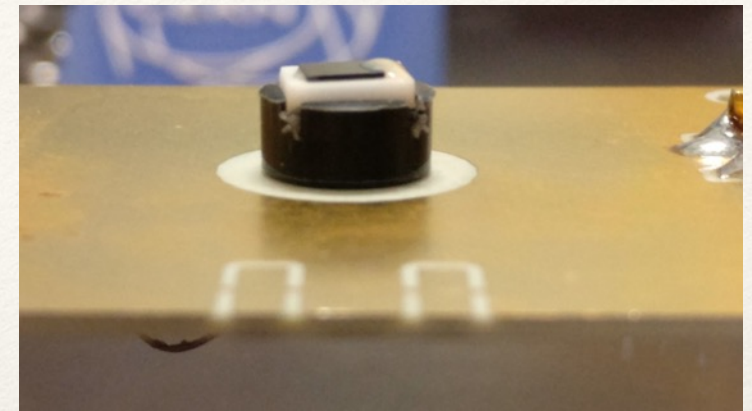
Type of measurements performed

- ❖ TCT
 - ❖ Front XY scans
 - ❖ Red and infrared
 - ❖ IR front voltage scans
- ❖ CV/IV



TCT Measurements

- ❖ Picosecond-pulse LASER (200 ps)
 - ❖ Red front (660 nm, $77 \mu\text{W}$ avg. peak power)
 - ❖ IR front (1064 nm, $137 \mu\text{W}$ avg. peak power)
- ❖ Customised bias T (C = 4.4 nF; R = 1 M Ω) + amplifier (effective amplification: 10 dB)
- ❖ Read-out and biasing from the back (cathode).

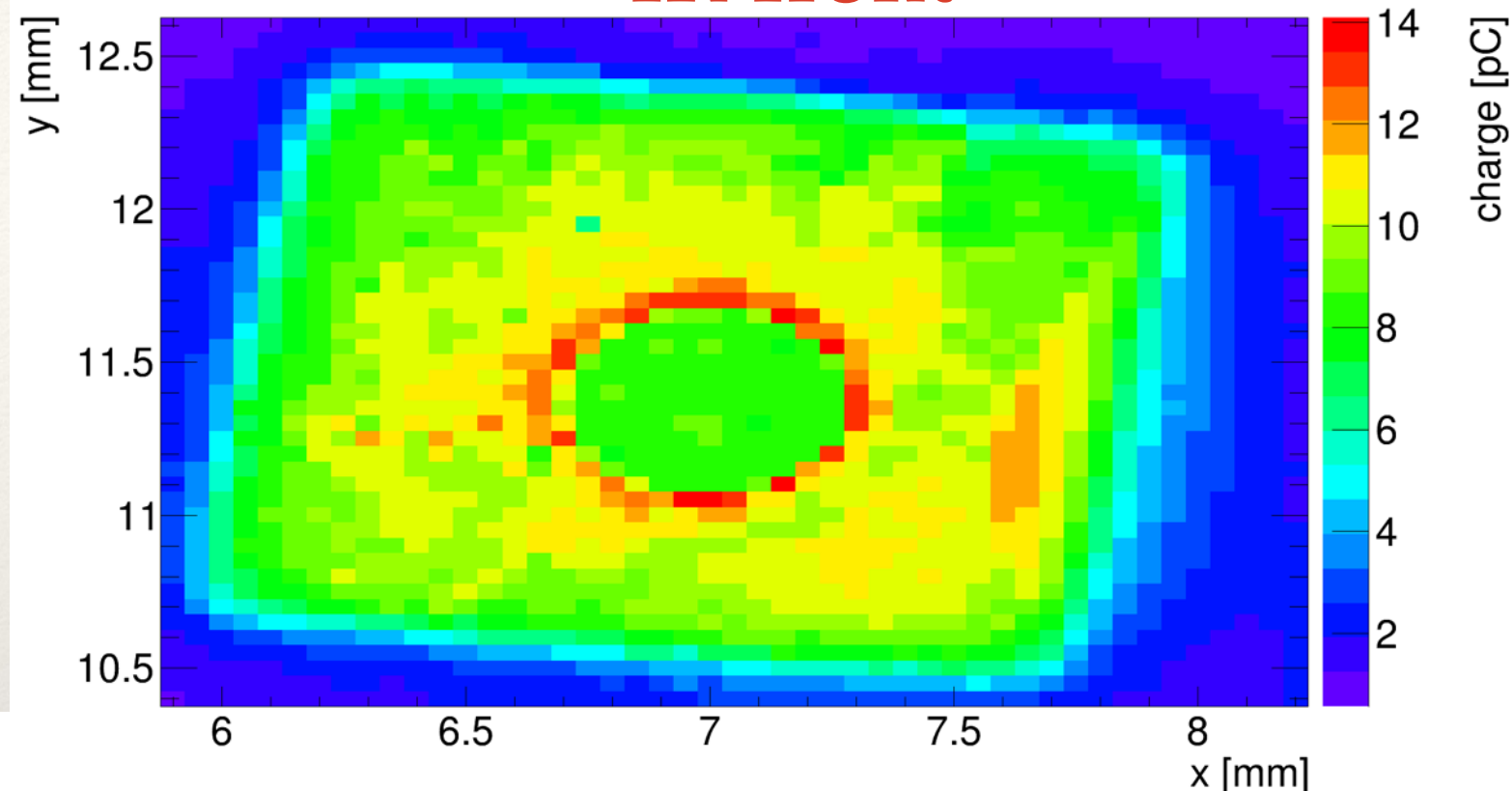


TCT XY SCANS

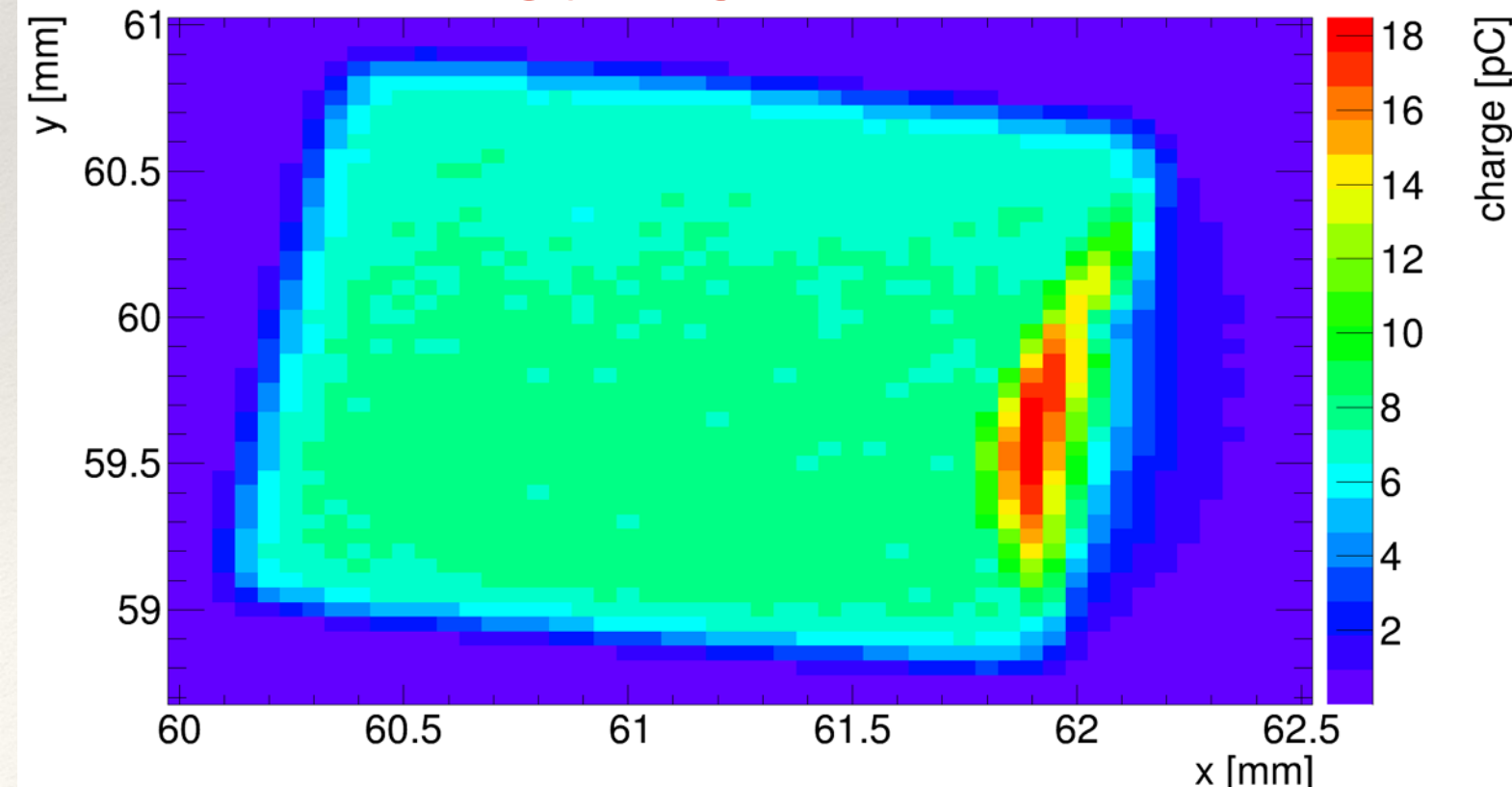
Unirradiated Sample

- ❖ Sample name: 394_1_7
- ❖ Red and IR front scans at 1700 V, 20°C
- ❖ Max. leakage current observed $\approx 0.05 \mu\text{A}$

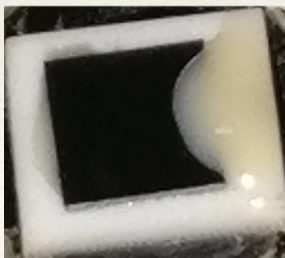
IR front



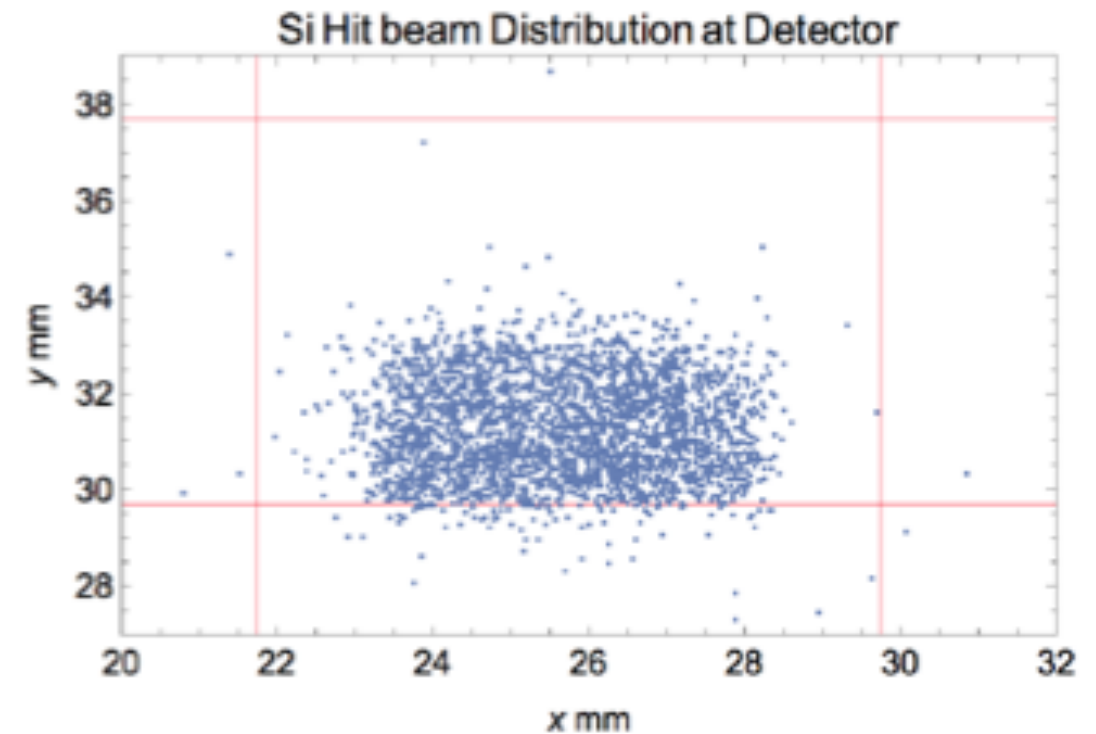
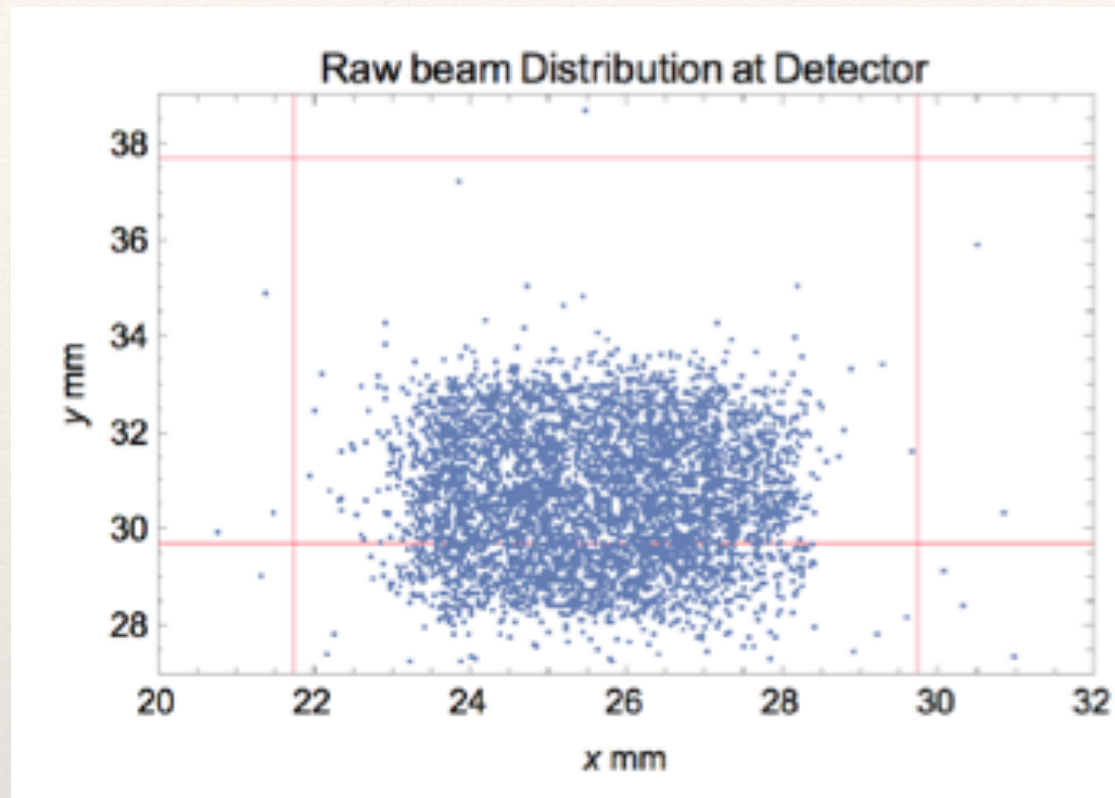
Red front



- ❖ Ring observed in IR scan
 - ❖ Optical effect cause by LASER reflection on the back connection.
- ❖ Right side inhomogeneity in red scan
 - ❖ Optical effect caused by reflections on glue blob.



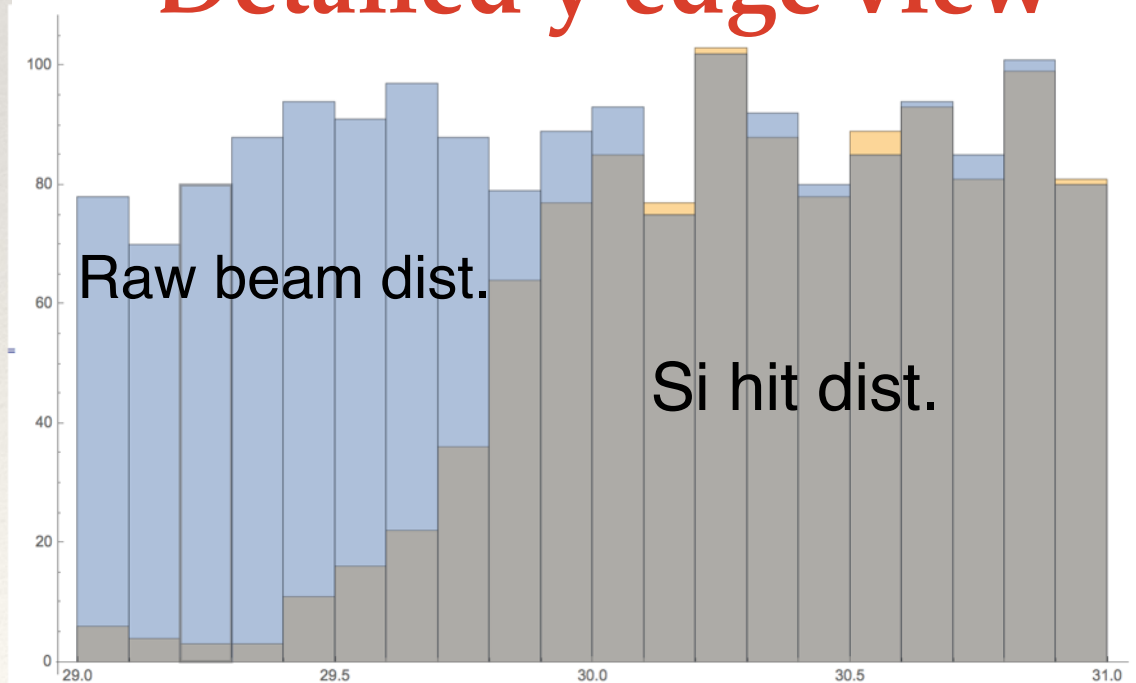
Unirradiated Sample



- ❖ Test beam results obtained on a HFS detector of different dimensions (8x8 mm) to that characterised in this presentation.
- ❖ Homogeneous particle detection.

(For more information see backup slides)

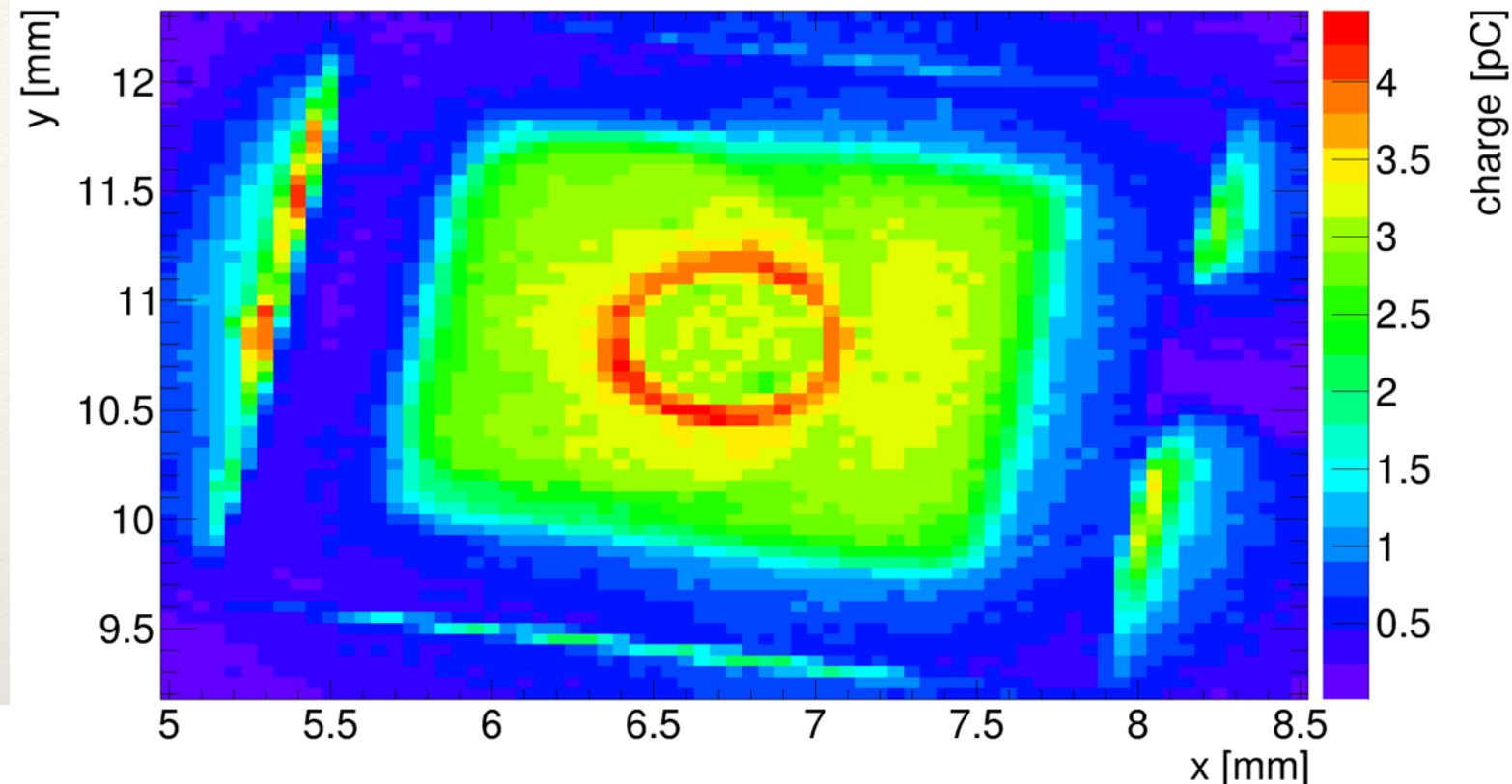
Detailed y edge view



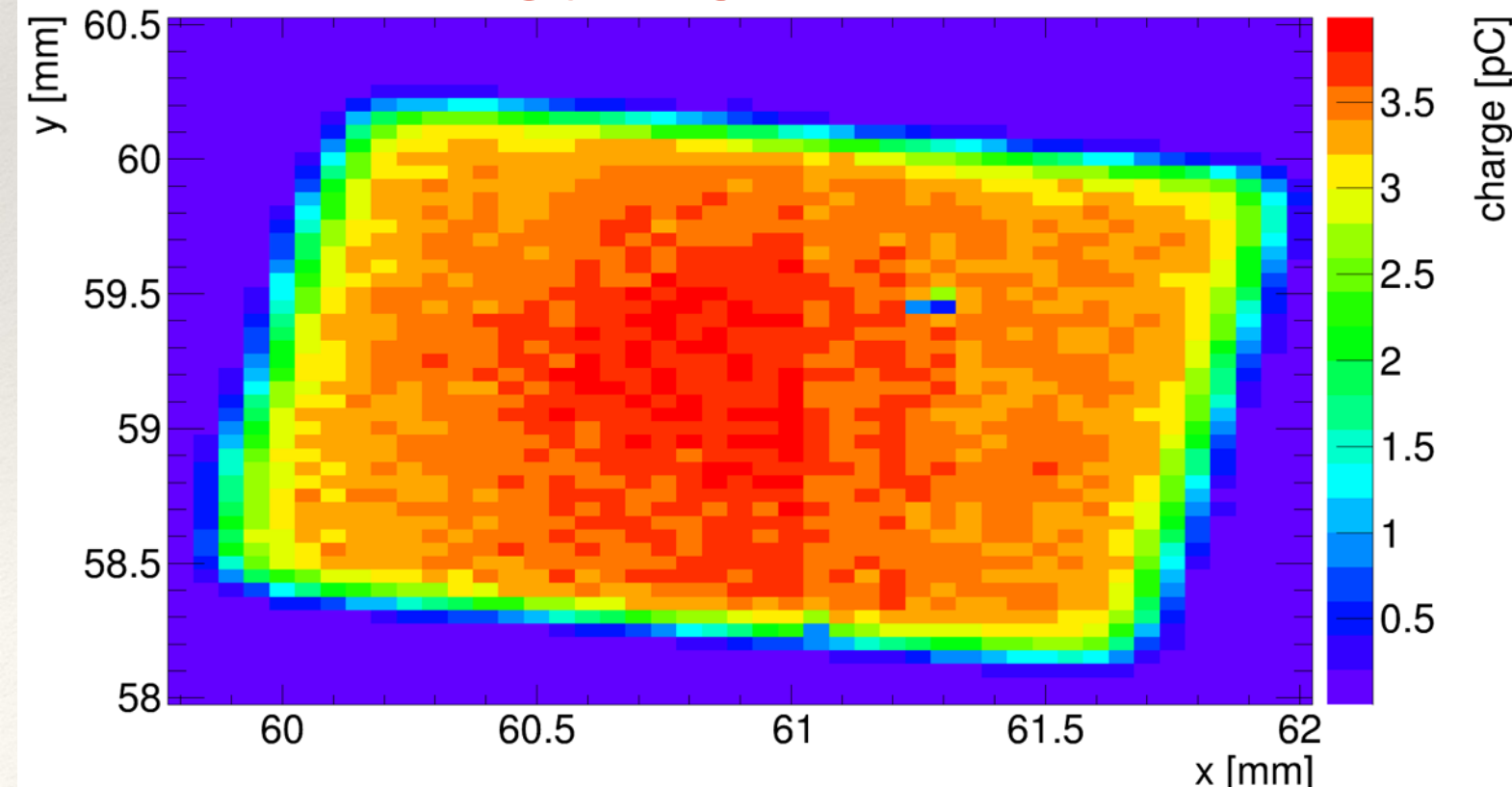
Irradiated $3\text{E}13 \text{ n/cm}^2$

- ❖ Sample name: 394_1_1
- ❖ Red and IR front scans at 1700 V, -20°C
- ❖ Max. leakage current observed $\approx 2.5 \mu\text{A}$

IR front



Red front

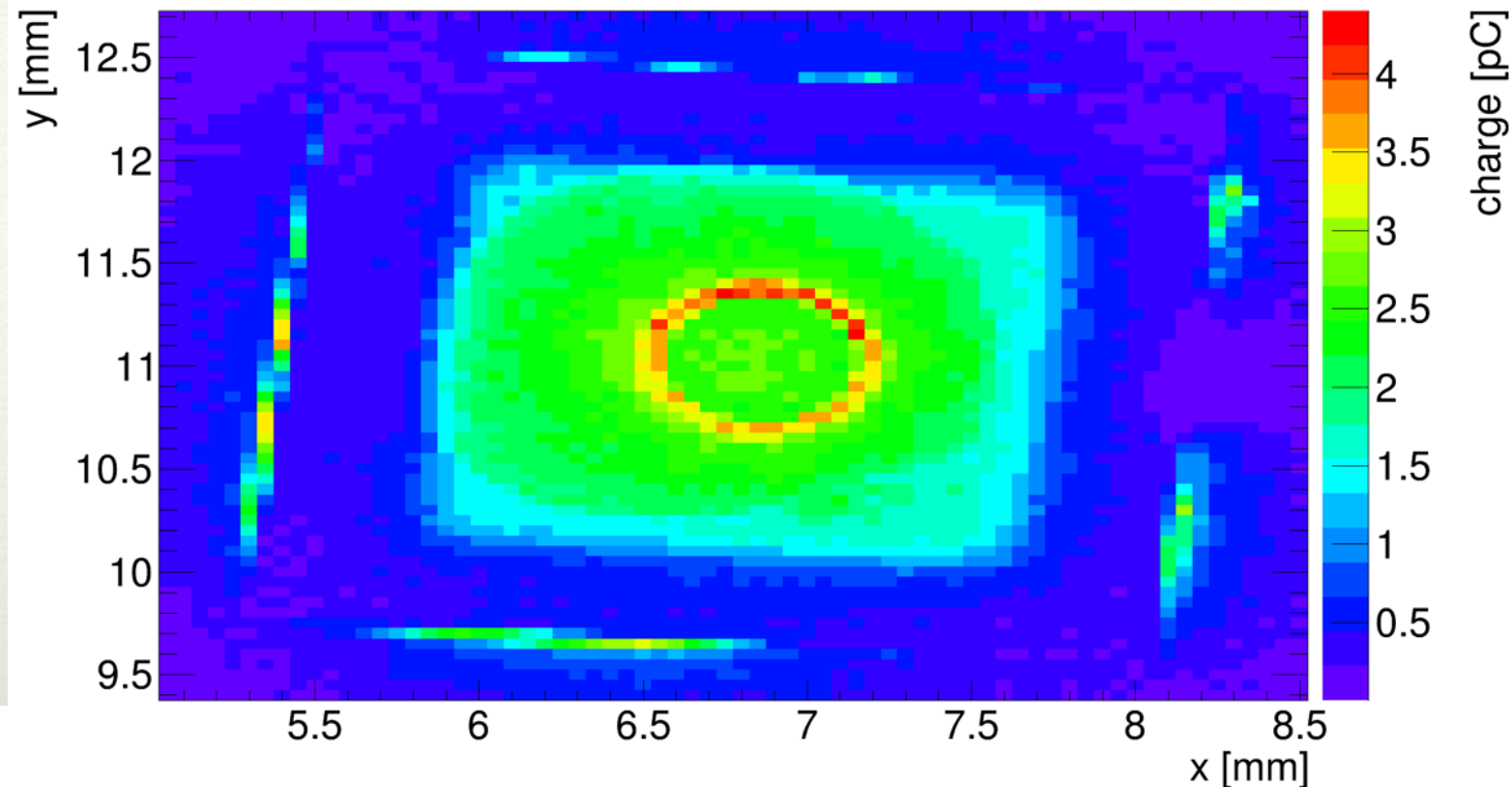


- ❖ The charge collection observed outside the sensor's active area on the IR scan is caused by reflections on glue surrounding the sensor (see backup slides).

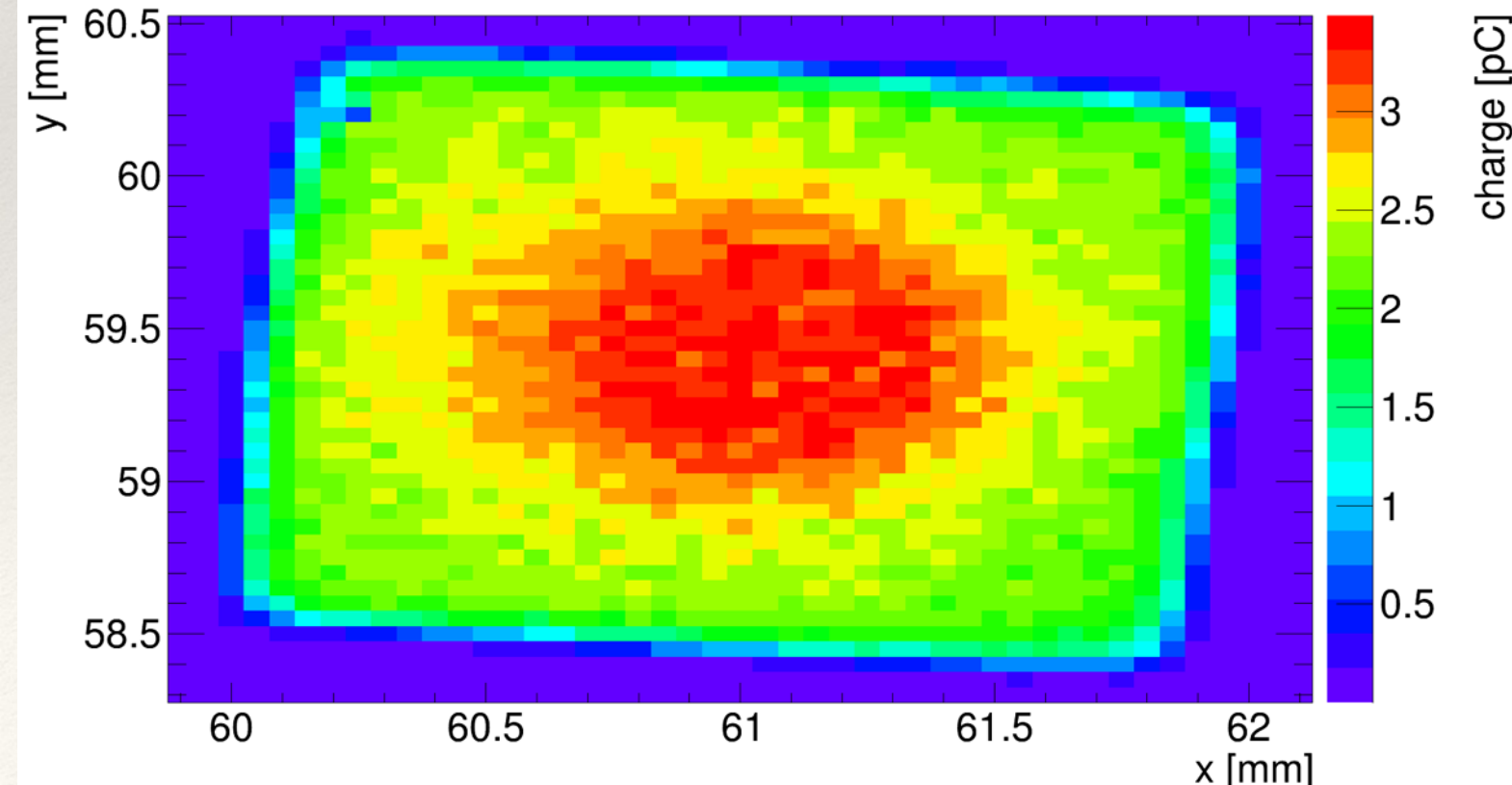
Irradiated 6E13 n/cm²

- ❖ Sample name: 394_1_3
- ❖ Red and IR front scans at 1700 V, -20°C
- ❖ Max. leakage current observed $\approx 2.0 \mu\text{A}$

IR front



Red front

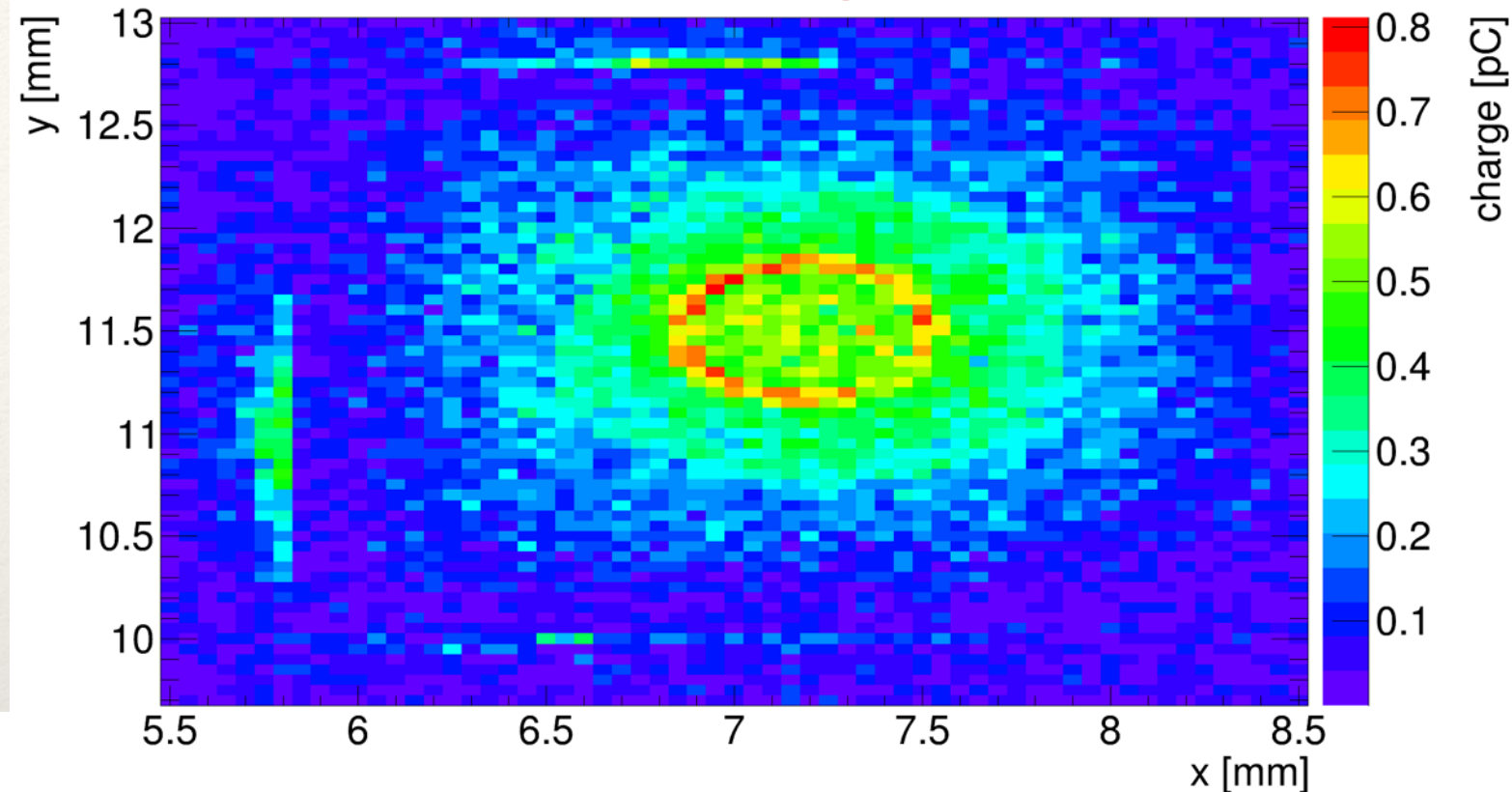


- ❖ Unexpected charge collection inhomogeneity in red scan.

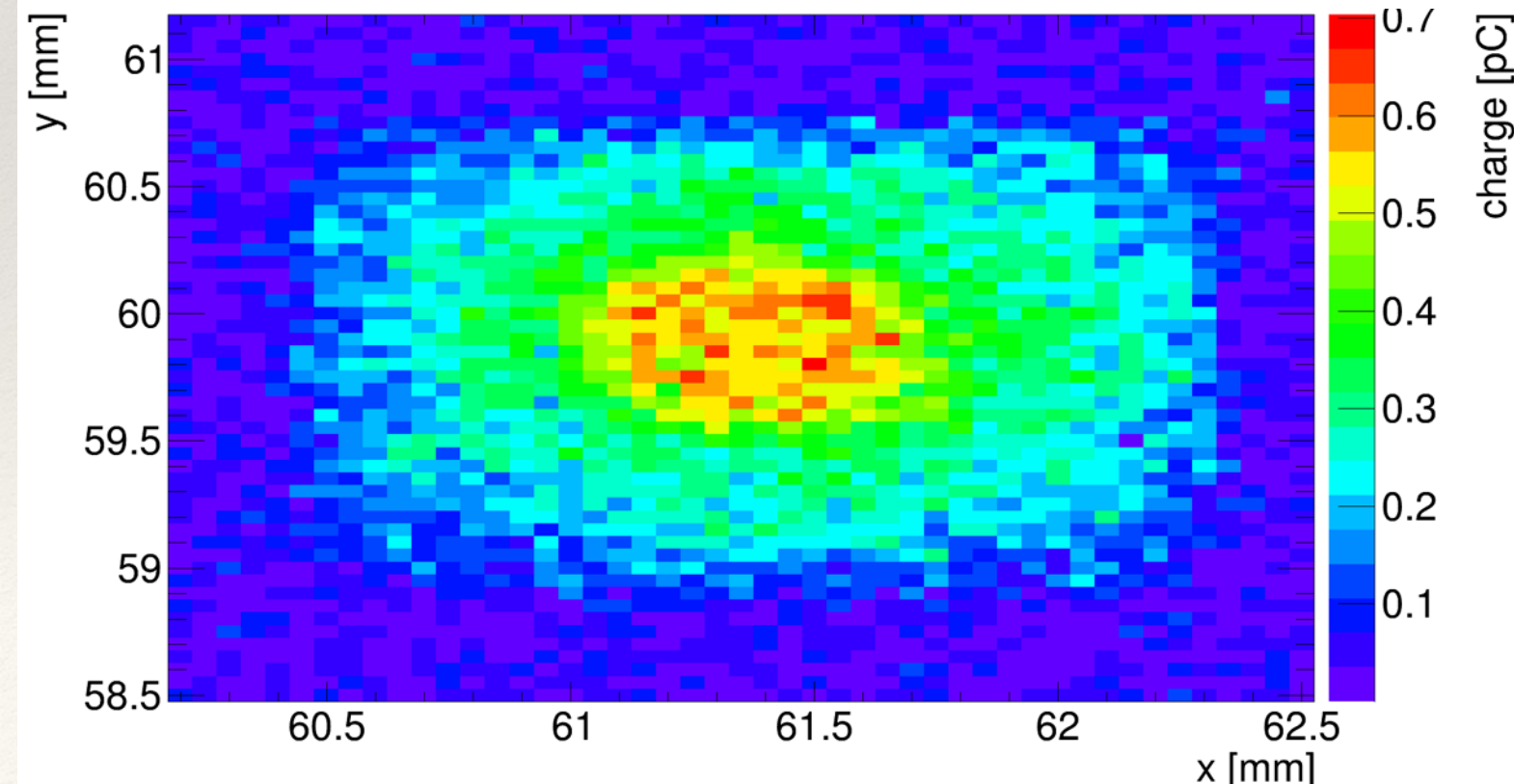
Irradiated $3\text{E}14 \text{ n/cm}^2$

- ❖ Sample name: 394_1_5
- ❖ Red and IR front scans at 1700 V, -20°C
- ❖ Max. leakage current observed $\approx 2.0 \mu\text{A}$

IR front



Red front



- ❖ Significant reduction of the active area.
- ❖ Unexpected charge collection inhomogeneity in red scan.

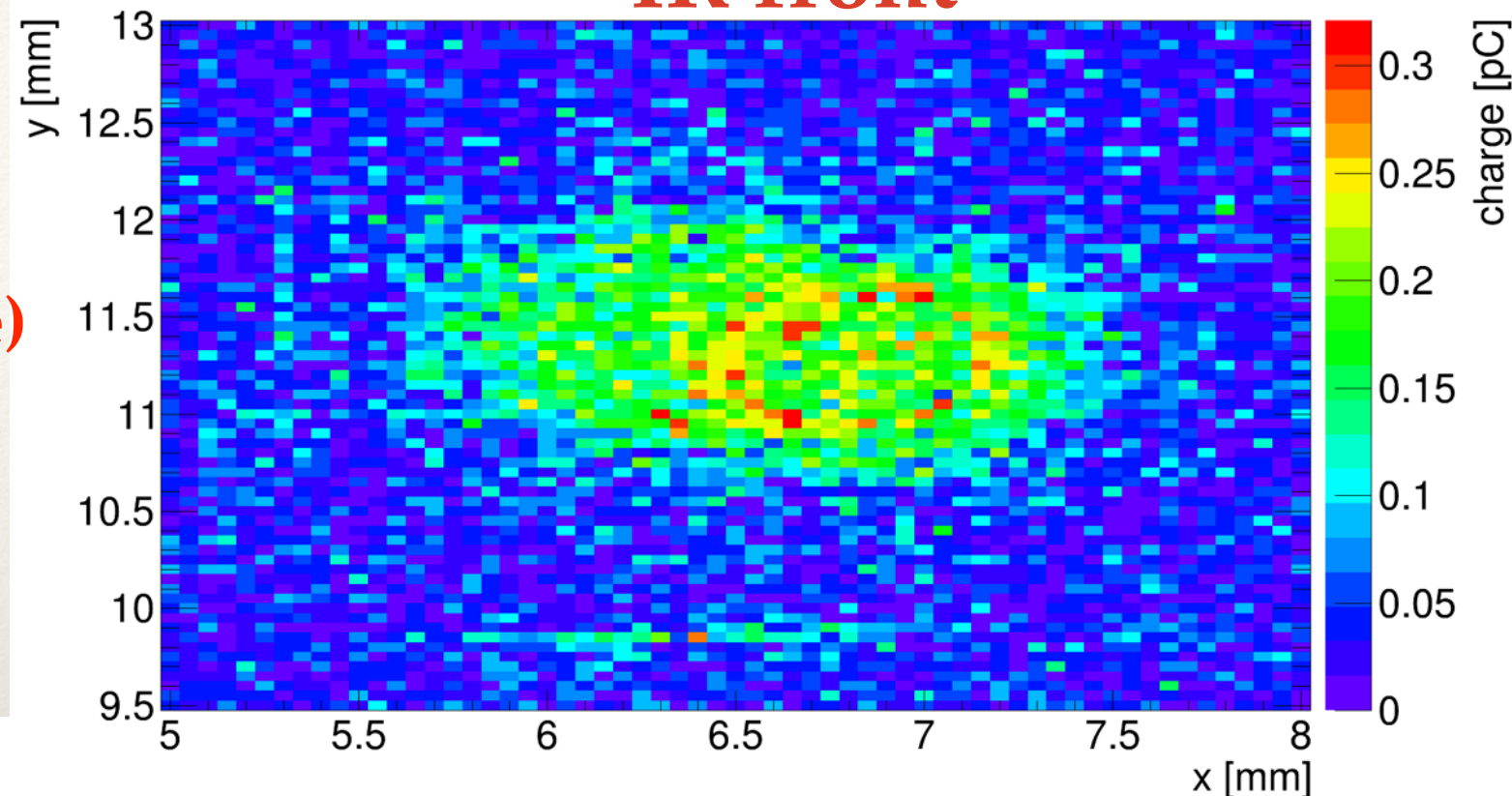
Irradiated $3\text{E}14 \text{ n/cm}^2$

❖ Sample name: 394_1_4

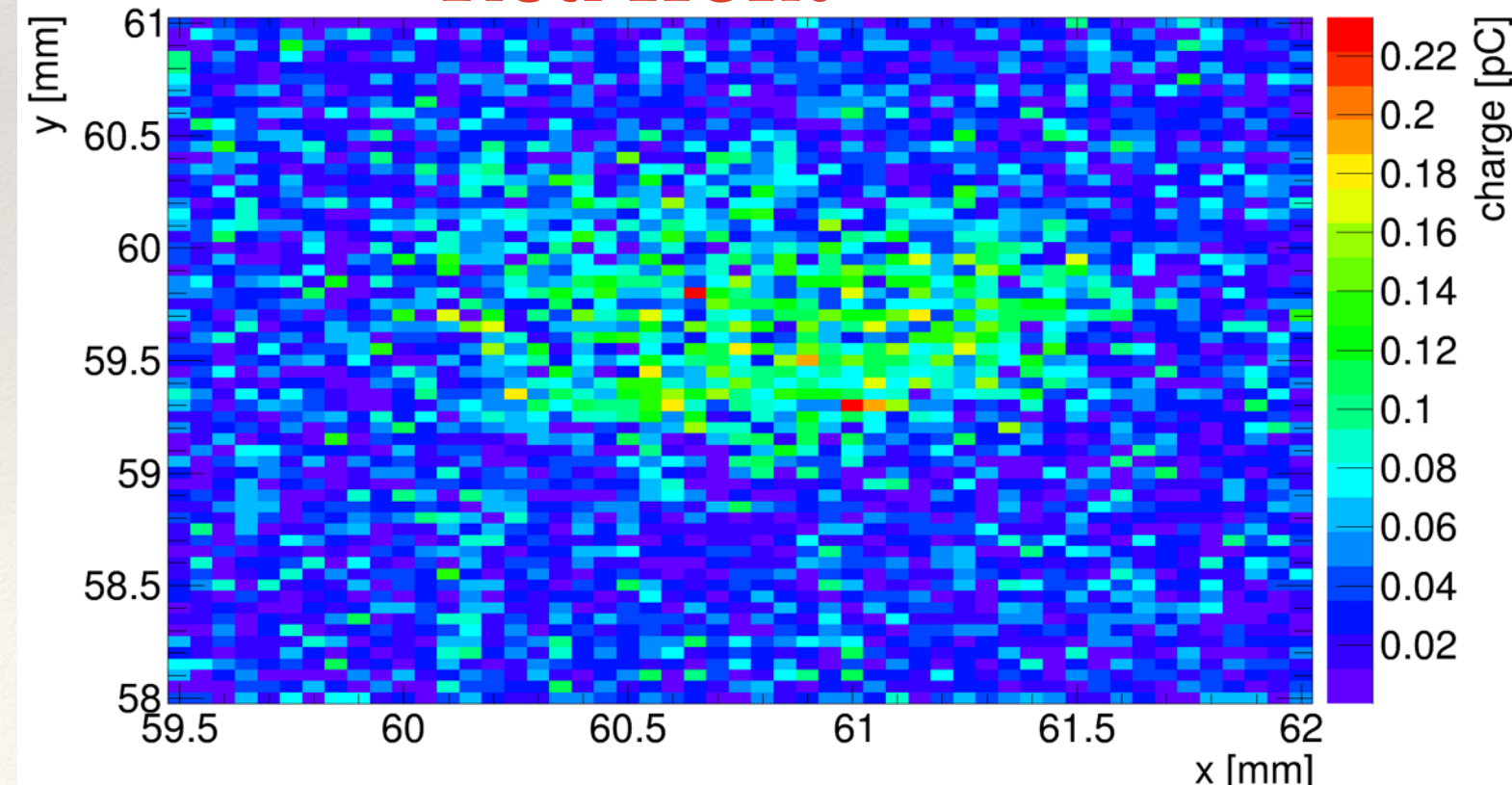
⚠ **At 1530 V leakage current: $10 \mu\text{A}$ (compliance)**

❖ Red and IR front scans at 1500 V, -20°C

IR front



Red front

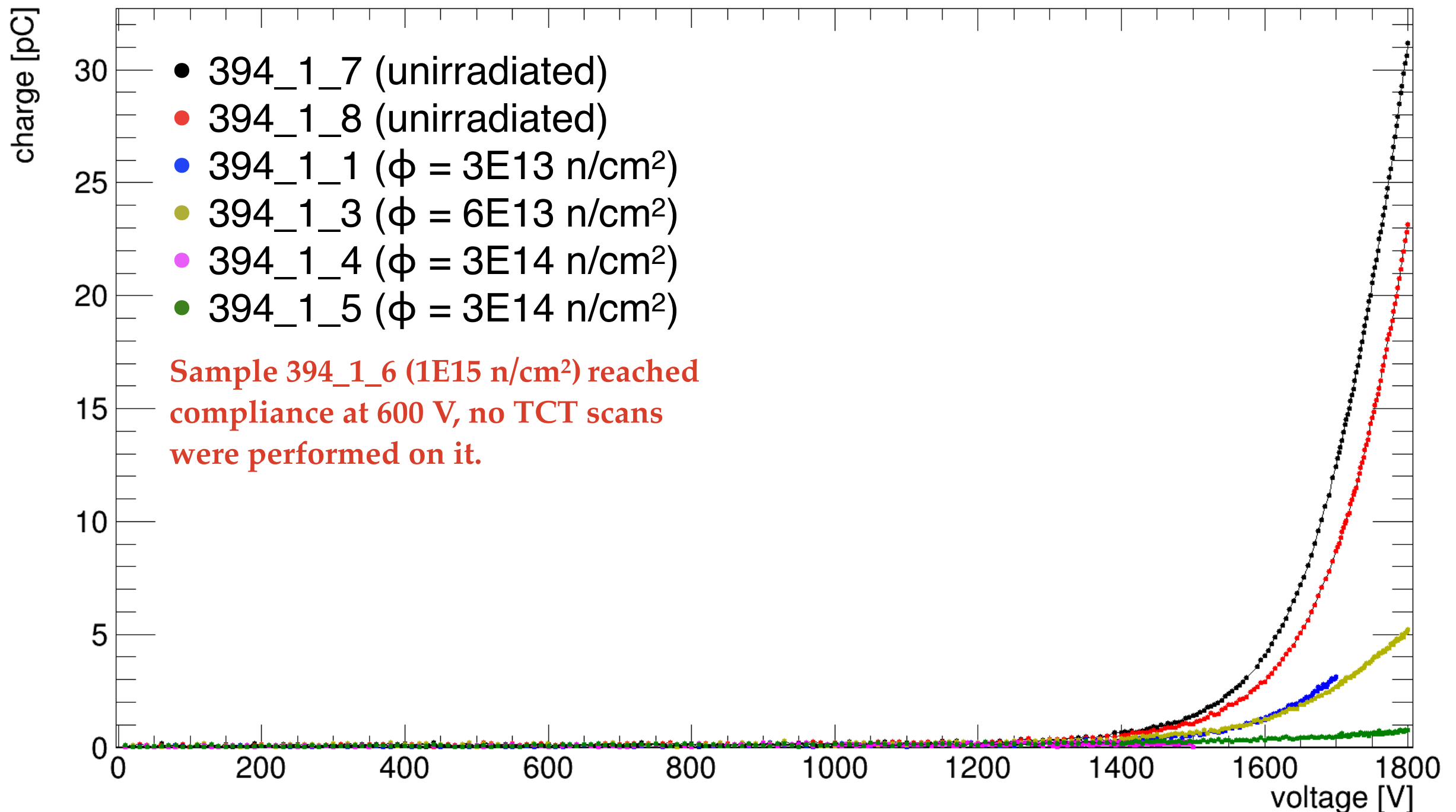


❖ Extreme reduction of the active area.

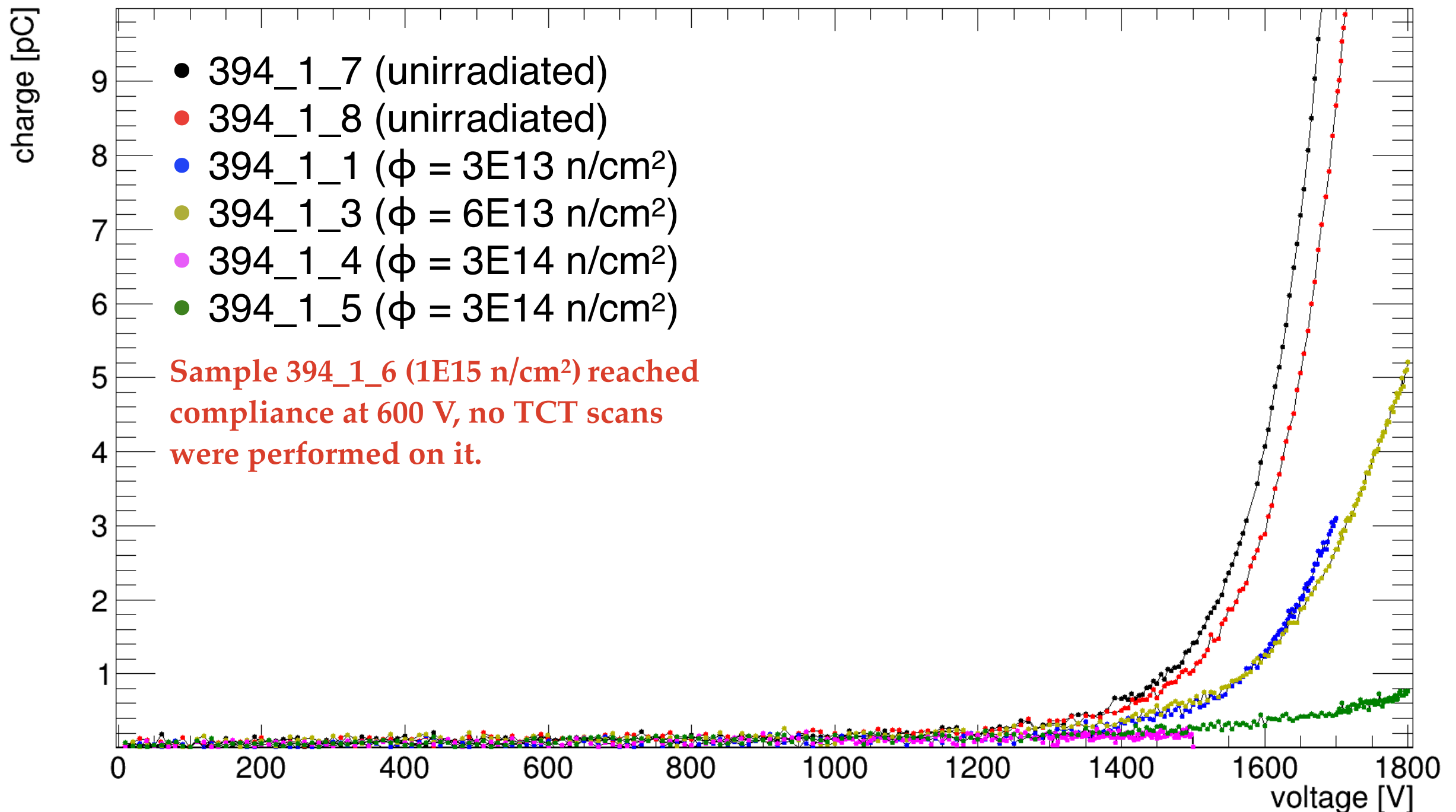
The sample irradiated up to $1\text{E}15 \text{ n/cm}^2$ reached compliance at 600 V, thus, no TCT scans were performed on it.

TCT VOLTAGE SCANS

Voltage Scans @ -20°C

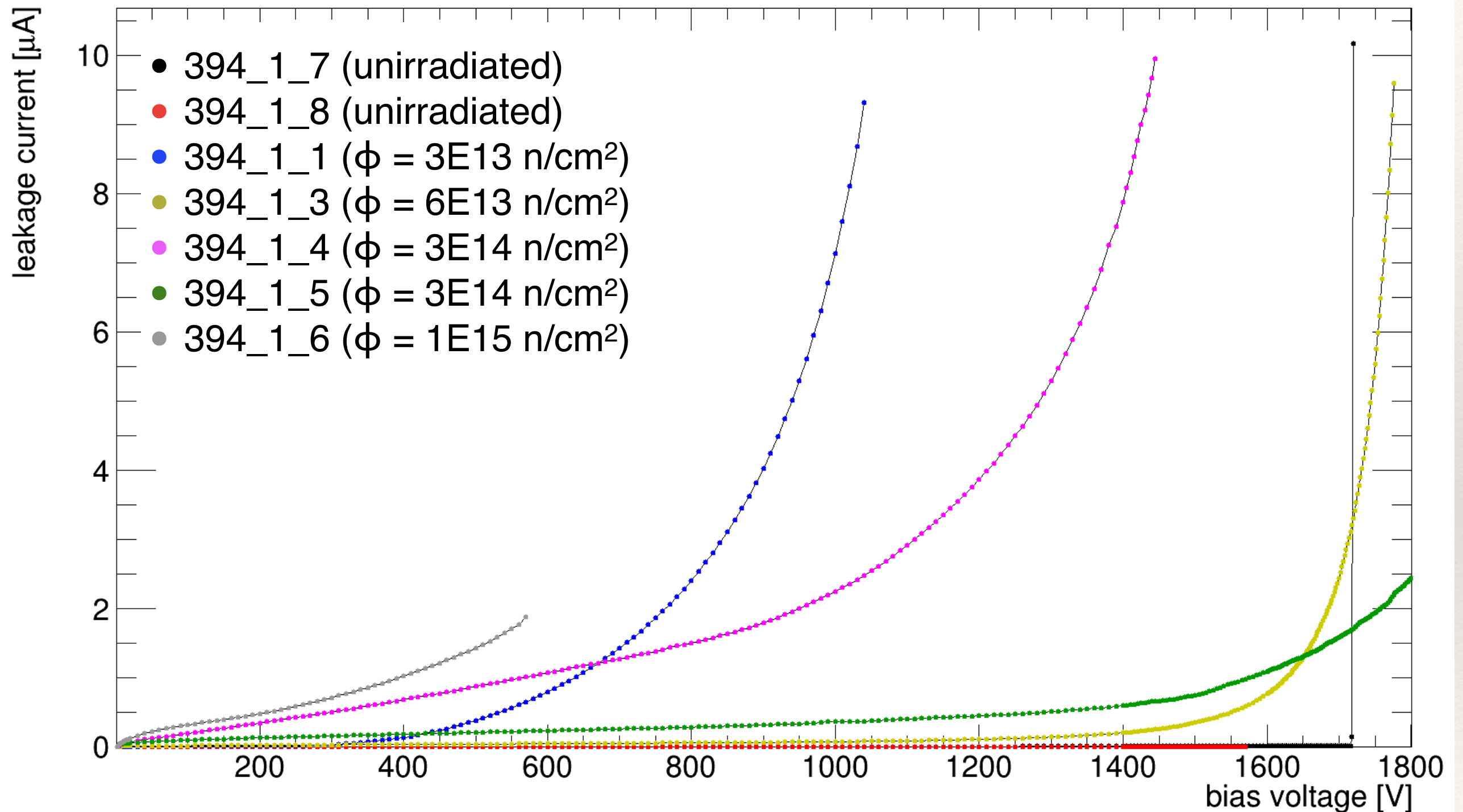


Voltage Scans @ -20°C



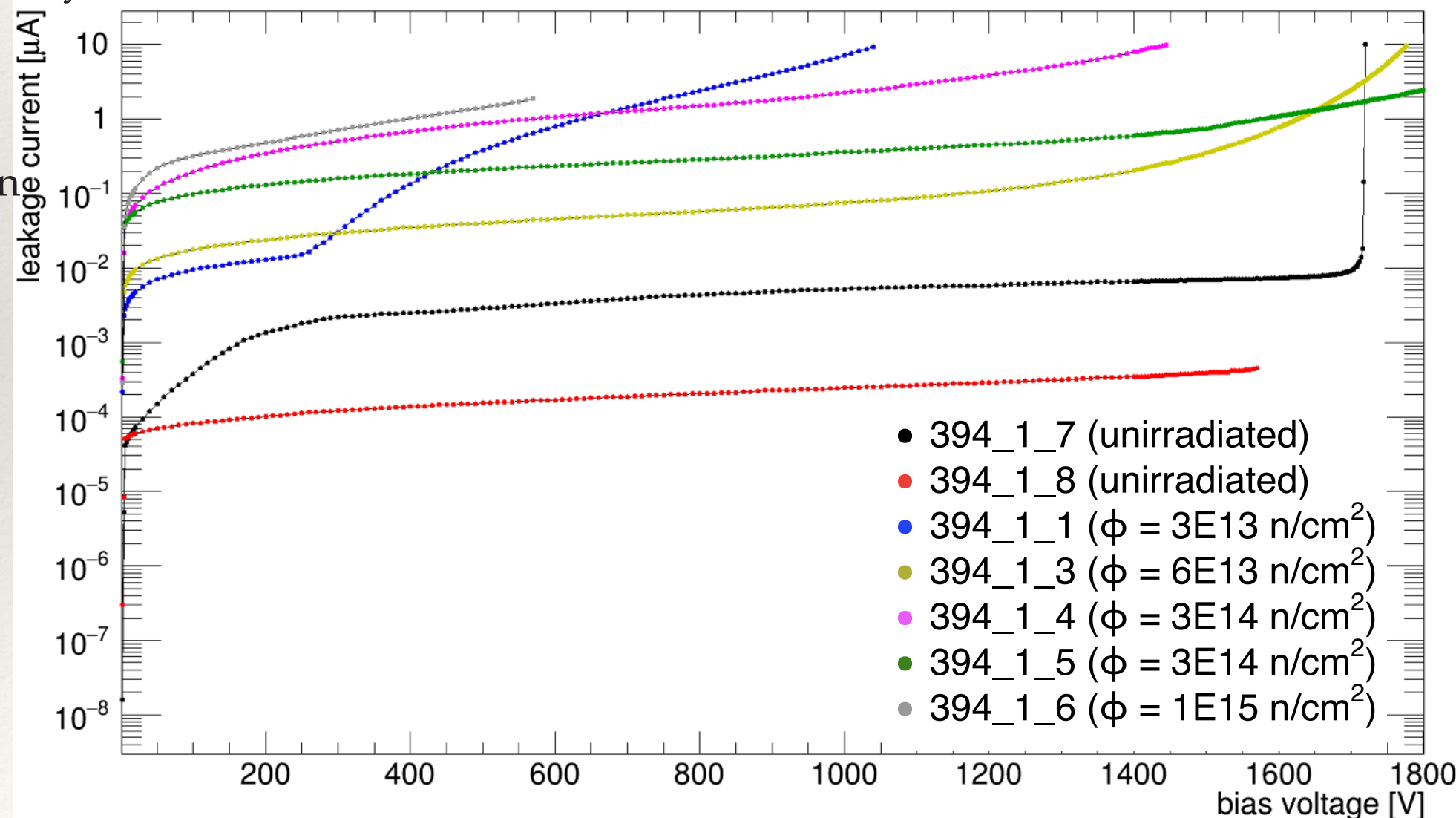
IV CURVES

IV Curves @ -20°C

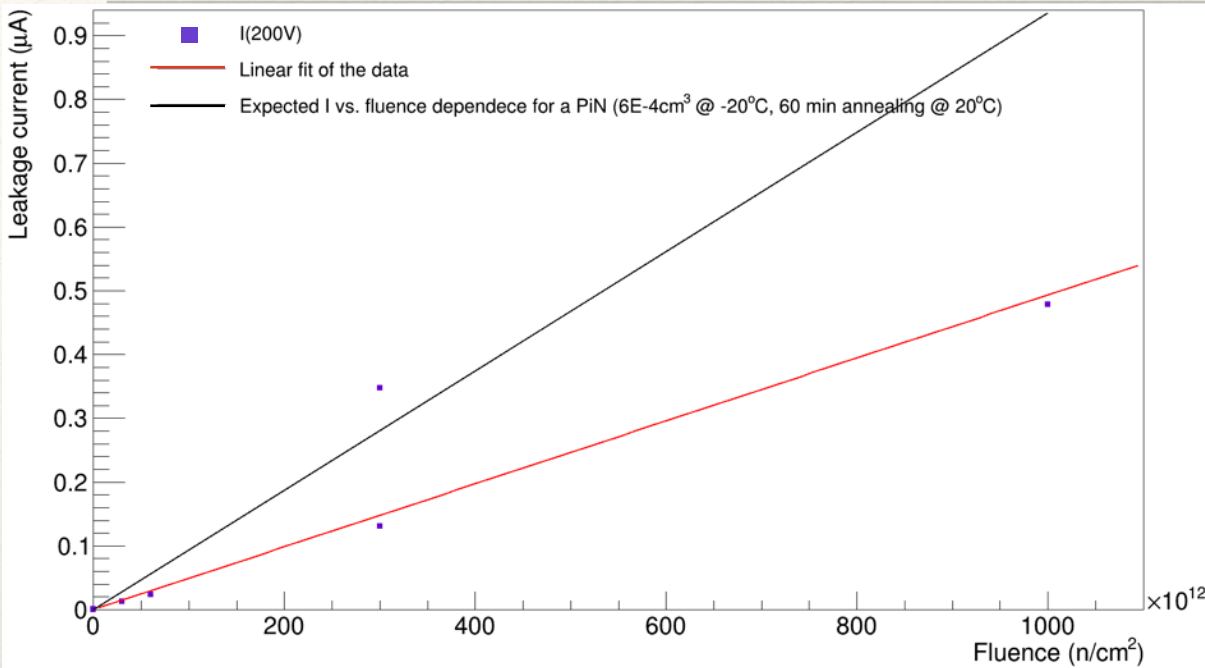


IV Curves @ -20°C

- ❖ Sample 394_1_3 suffered a change in breakdown voltage with respect to when TCT measurements were performed.
 - ❖ Possible explanation: damage to the cathode and/or anode connections.
- ❖ Samples 394_1_4 and 395_1_5 (both irradiated to $3\text{E}14 \text{ n/cm}^2$) behave differently.
- ❖ Also, the two unirradiated samples behave differently.
 - ❖ Possible explanation given by RMD: the sensors could be from different wafers which also means there could be differences in:
 - Doping profile
 - Depth of the PN junction
 - Thickness of the sensor



I(200 V) vs. Fluence @ -20°C



Damage coefficient:

- ❖ From fitting HFS data:
 $\alpha_{\text{fit}} \approx 8.22\text{E-}19 \text{ A/cm}$
- ❖ For a PiN with equal volume and annealing:
 $\alpha_{\text{PiN}} \approx 15.6\text{E-}19 \text{ A/cm}$

ESTIMATION

Active volume changes are not being considered.

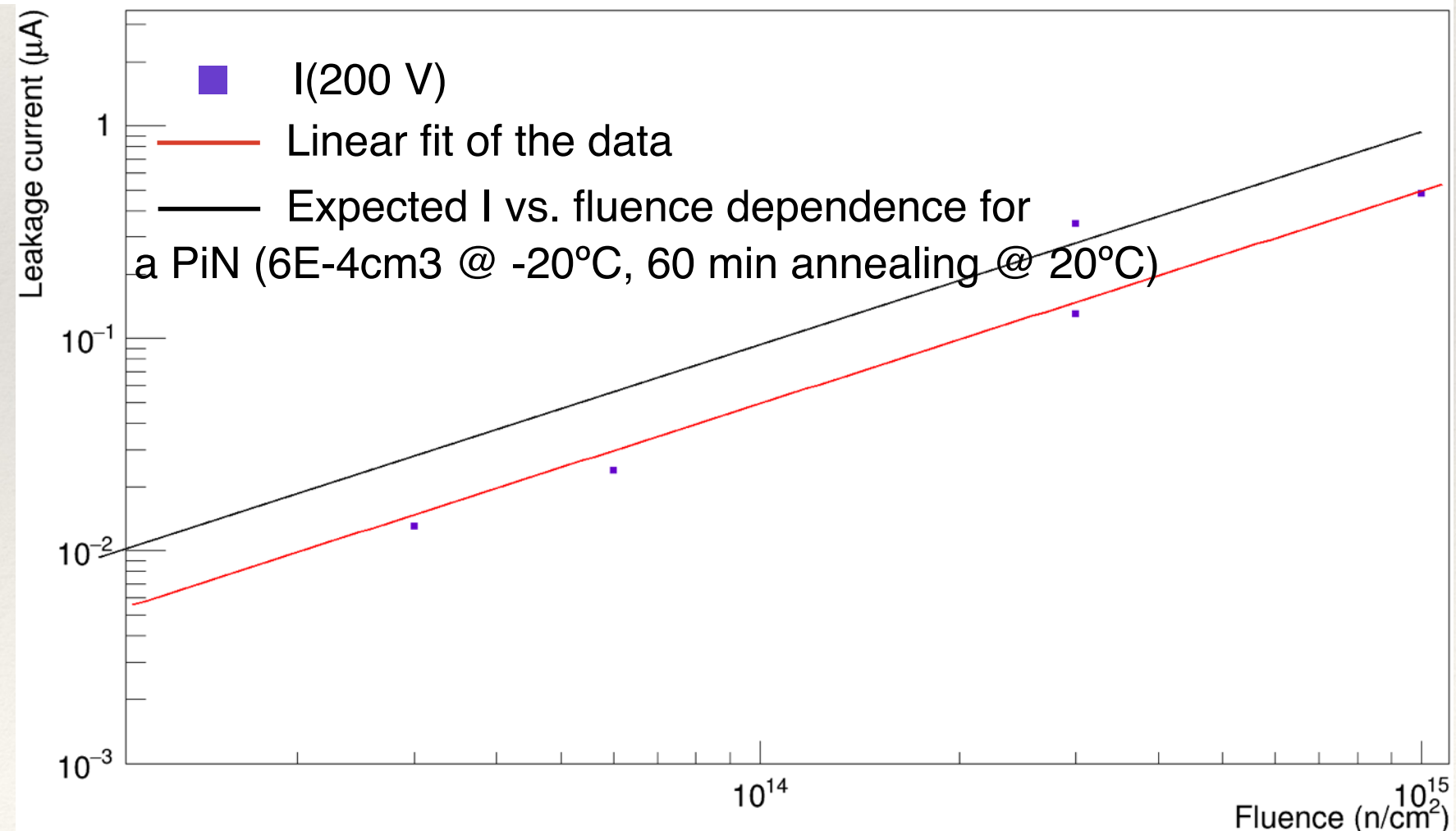
Dimensions assumed:

Active area: 2x2 mm

Thickness: 120 μm

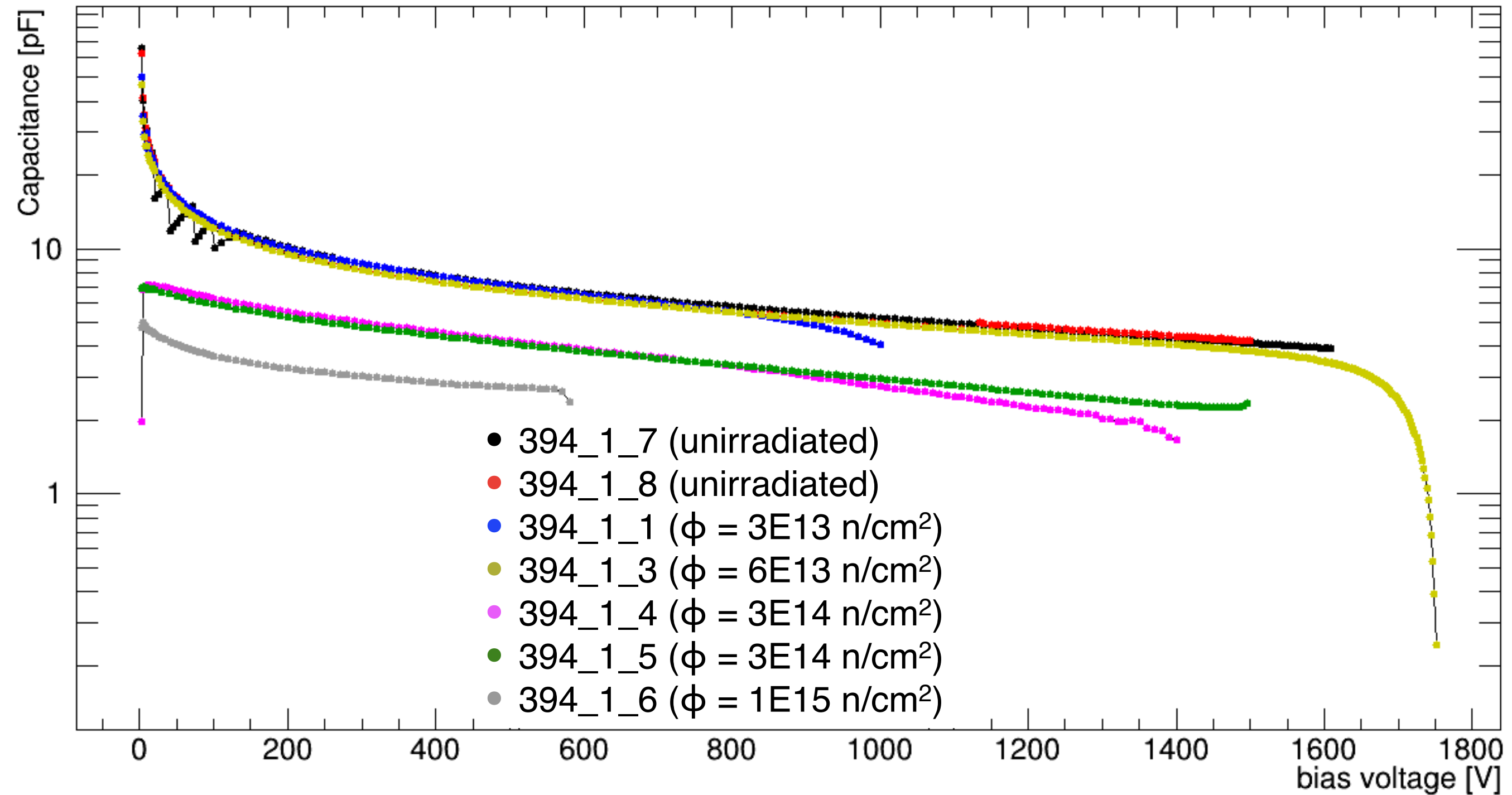
Estimated annealing:

60 min @ 20°C



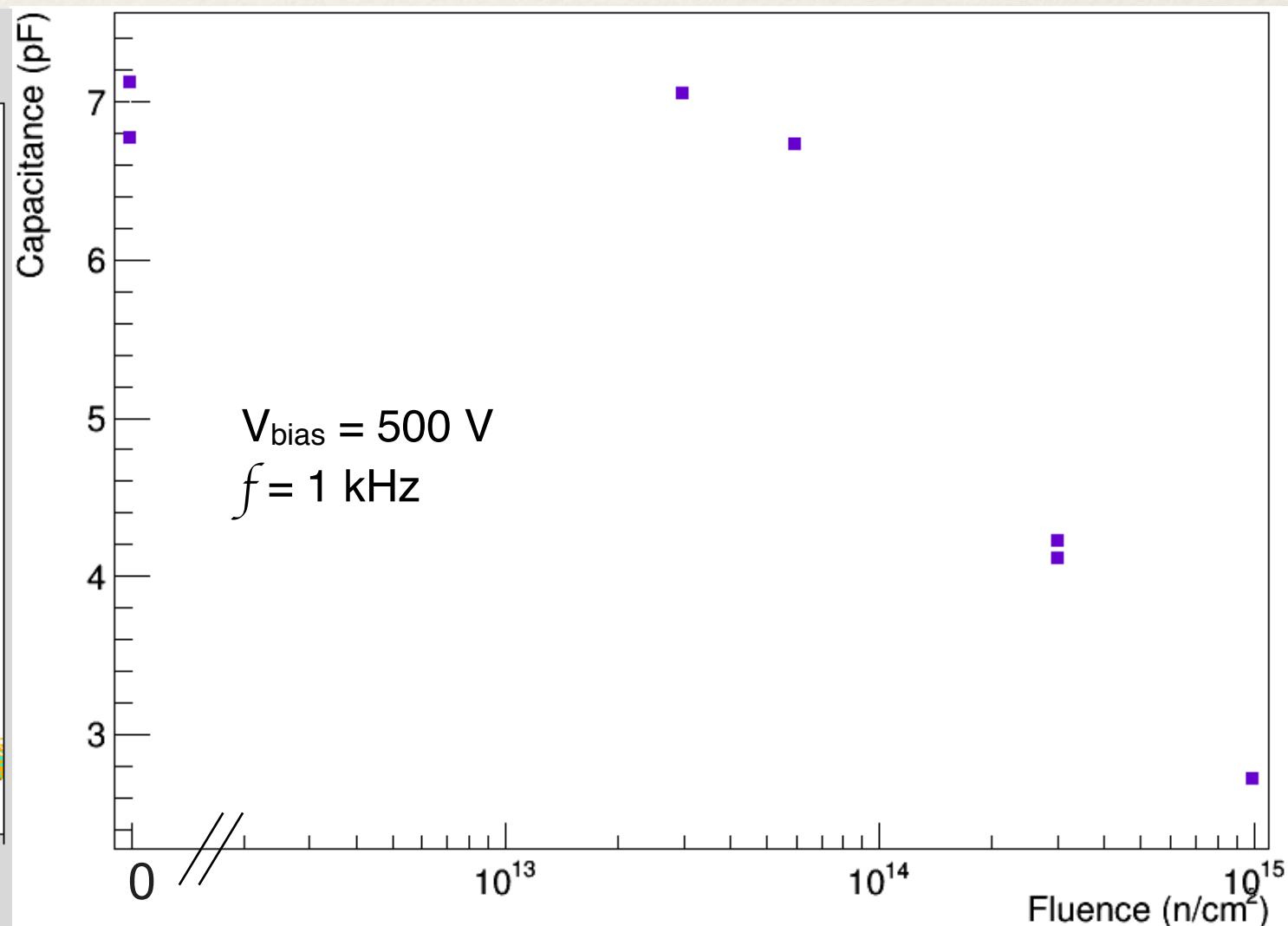
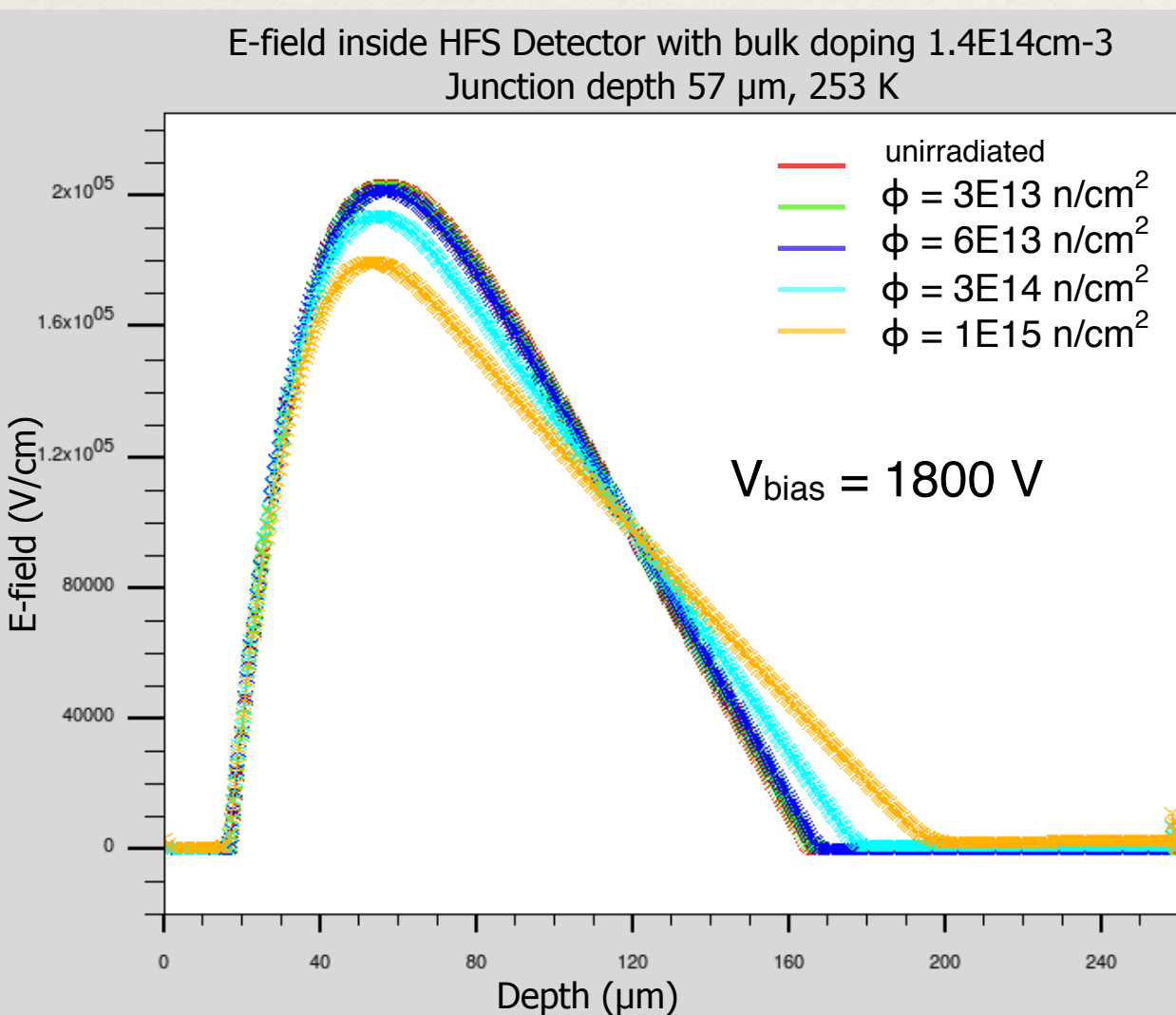
CV CURVES

CV Curves @ -20°C



CV Curves @ -20°C

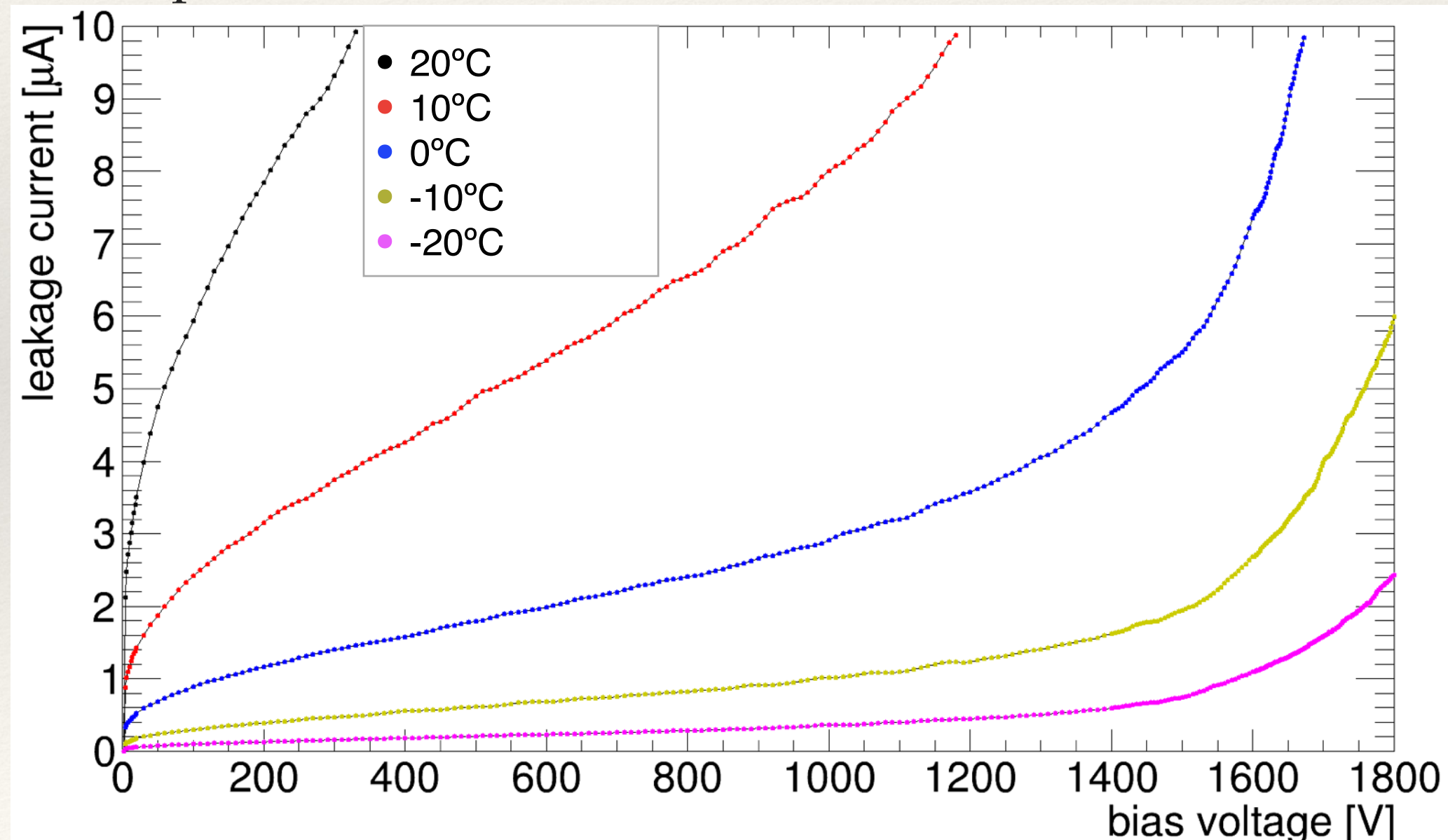
- ❖ Capacitance decreases with fluence.
- ❖ Equivalent to an increase in thickness of the depletion region.
- ❖ Same tendency as the simulations done on TCAD by the Delhi group.



IV vs. T

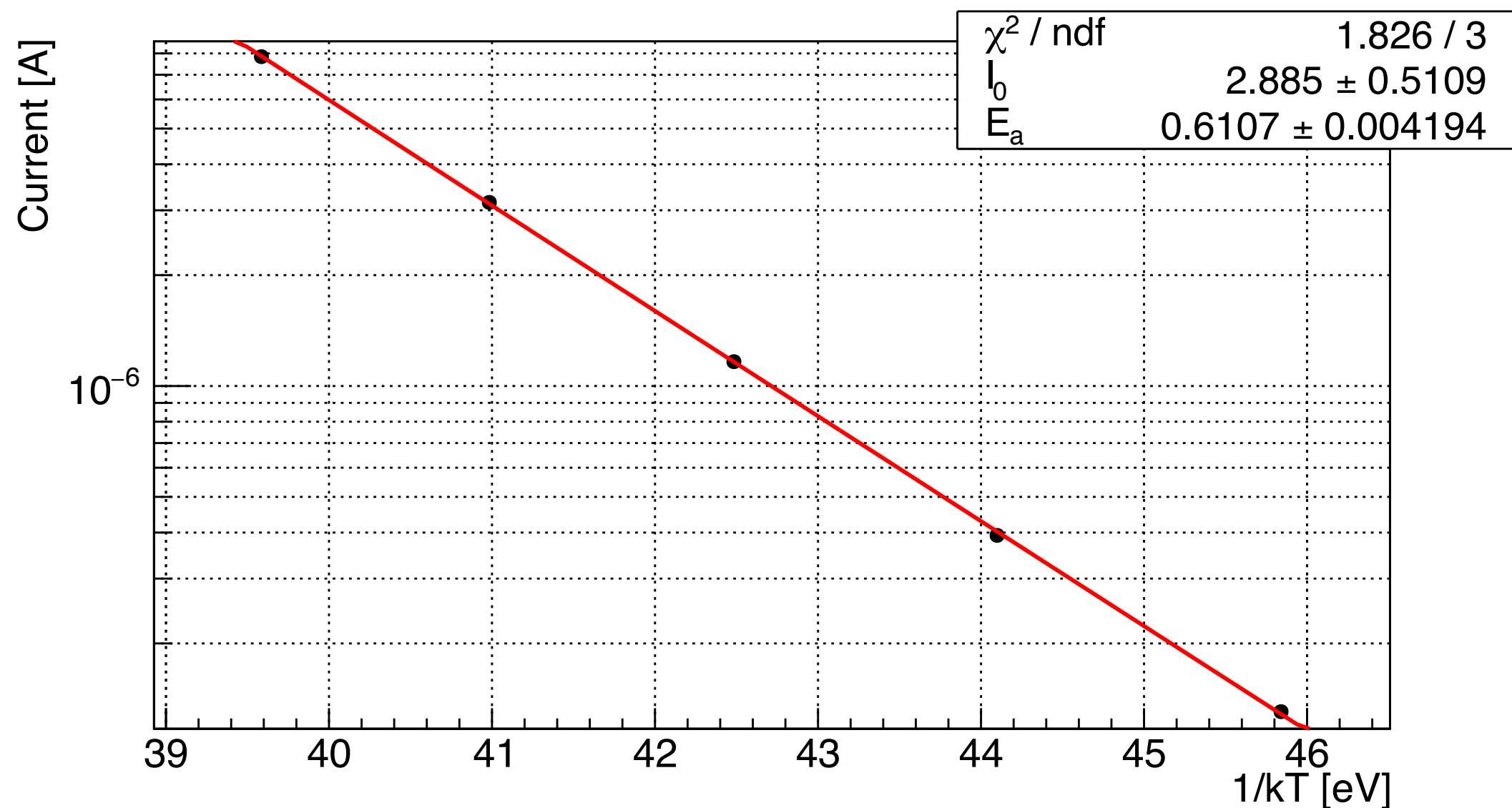
IV Curves @ Different Temperatures

- ❖ Sample 394_1_5, $\phi = 3\text{E}14 \text{ n/cm}^2$.
- ❖ IV curves were measured at 5 different temperatures.
- ❖ Objective: produce an Arrhenius plot, calculate the activation energy and compare it with the expected value.



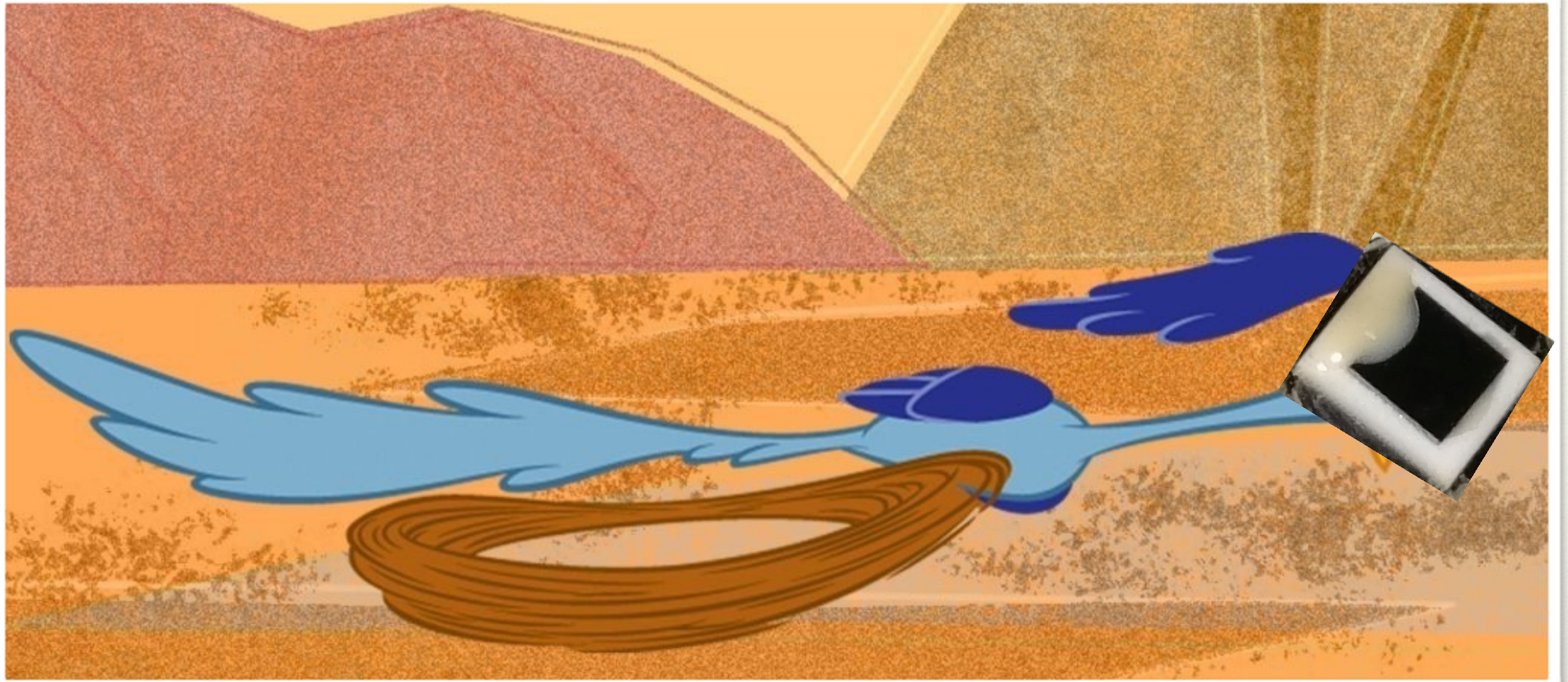
Arrhenius Plot

- ❖ Sample 394_1_5, $\phi = 3\text{E}14 \text{ n/cm}^2$, $I(200\text{V})$.
- ❖ Result from the fit: $E_{\text{ef}}^{\text{fit}} \approx 1.22 \text{ eV}$.
- ❖ Expected result: $E_{\text{ef}} \approx 1.21 \text{ eV}$. [2013, A. Chilingarov, JINST 8 P10003]



Conclusions

- ❖ TCT XY scans on unirradiated samples show inhomogeneities due to purely optical effects
 - ❖ These inhomogeneities are not seen with particles (test beam results).
- ❖ TCT XY scans show an apparent reduction with fluence of the active area of the sensors.
- ❖ A central inhomogeneity appears in the red laser scans of samples irradiated to a $\phi \geq 6E13 \text{ n/cm}^2$.
 - ❖ This has yet to be understood.
- ❖ TCT voltage scans show a decrease in charge collection with fluence.
- ❖ From the IV measurements @ 200 V (gain=1) it was possible to estimate α ($8.22E-19 \text{ A/cm}$), which resulted of the expected order of magnitude.
- ❖ CV measurements show an increase in the depletion region thickness with fluence.
 - ❖ In agreement with simulations.
- ❖ Variation in CV/IV and TCT observed between different samples:
 - ❖ For two non irradiated samples
 - ❖ For two samples irradiated to the same fluence ($3E14 \text{ n/cm}^2$)
 - ❖ RMD stated this could be due to the samples coming from different wafers.
 - ❖ **It is crucial to measure and test all samples before an irradiation campaign.**
- ❖ **We must study a new set of detectors in order to have a better understanding of their behaviour.**
 - ❖ We already have the samples and work will begin in the following weeks.

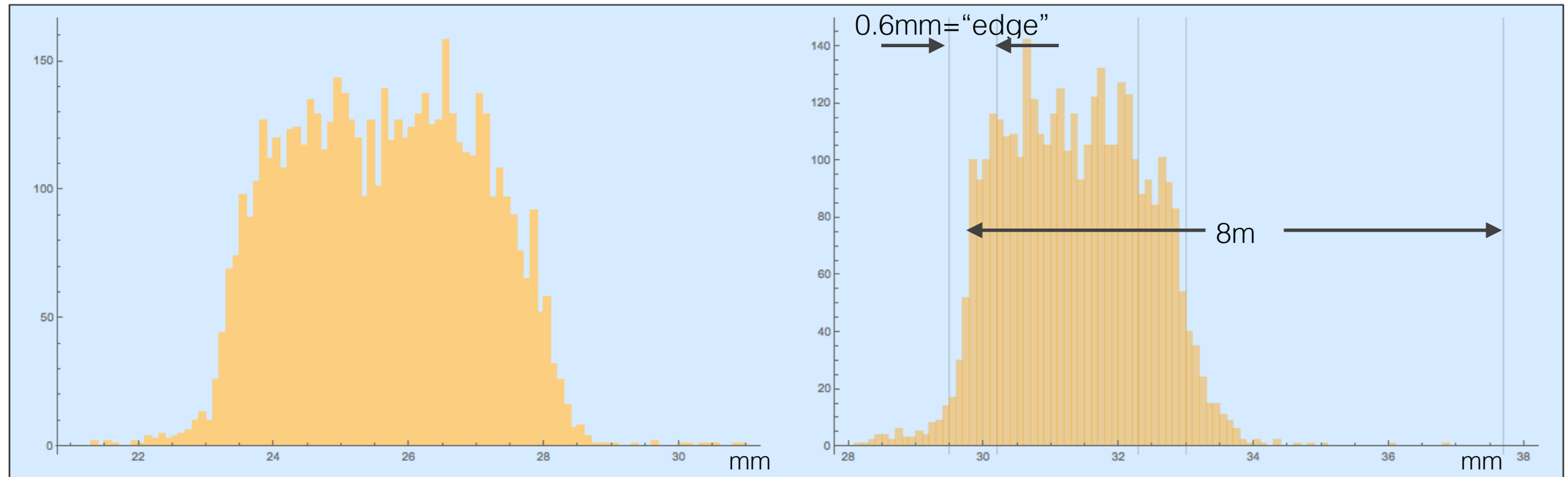


Thank you

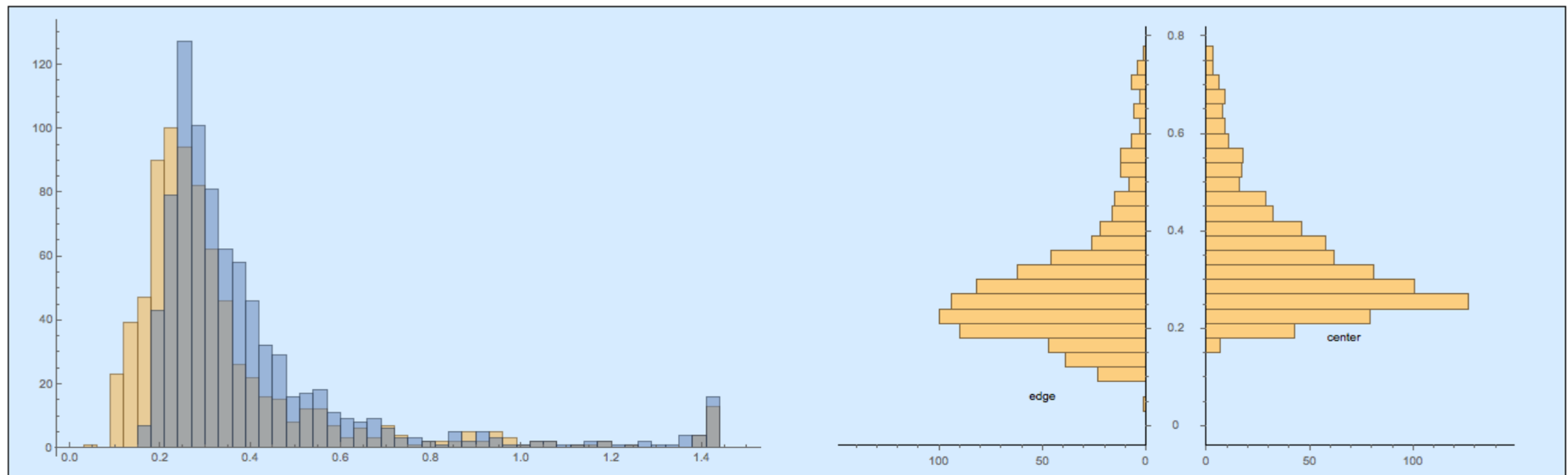
BACKUP SLIDES

8x8 HFS Hit Distribution - Test Beam Results

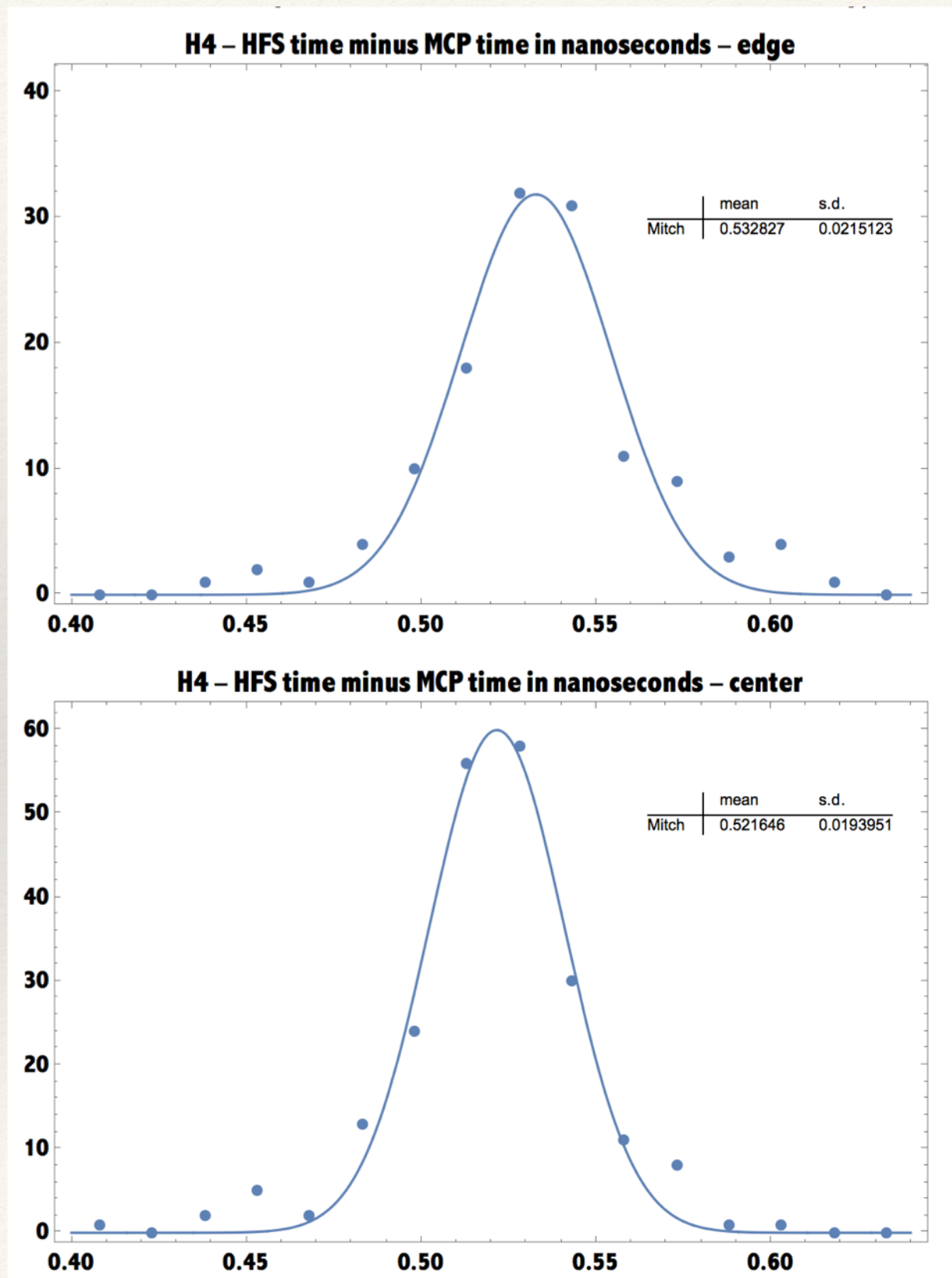
x ,y profile (in mm) of valid hits, Gridlines show selection for edge, center and top of Si



HFS Peak Amplitude in Volts, at detector edge compared w. center

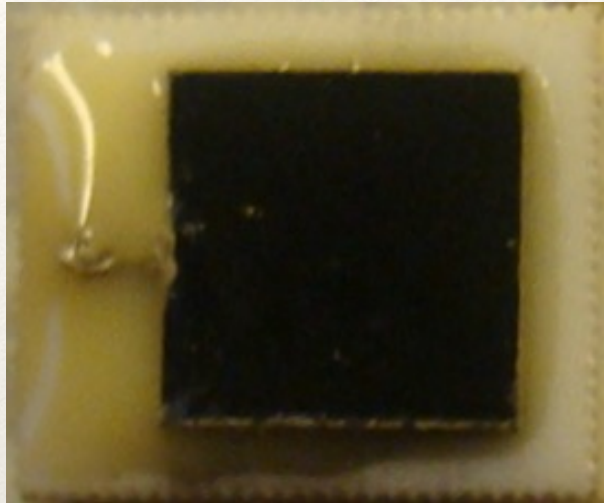


Very Preliminary Look at Timing on Detector Edge

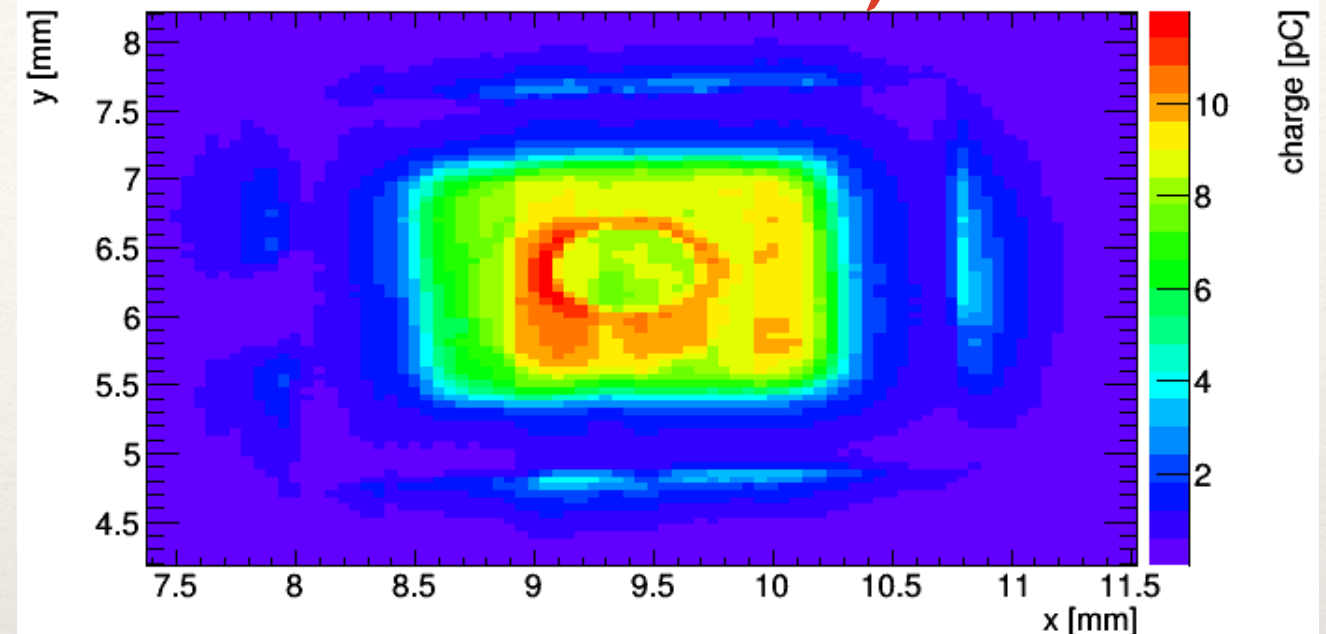


- ❖ Due to the complicated edge structure of this high field Si, it was difficult to evaluate w.
- ❖ First look at edge behaviour is encouraging.
- ❖ The timing algorithm is still preliminary.
 - ❖ Small pulse height distortion.

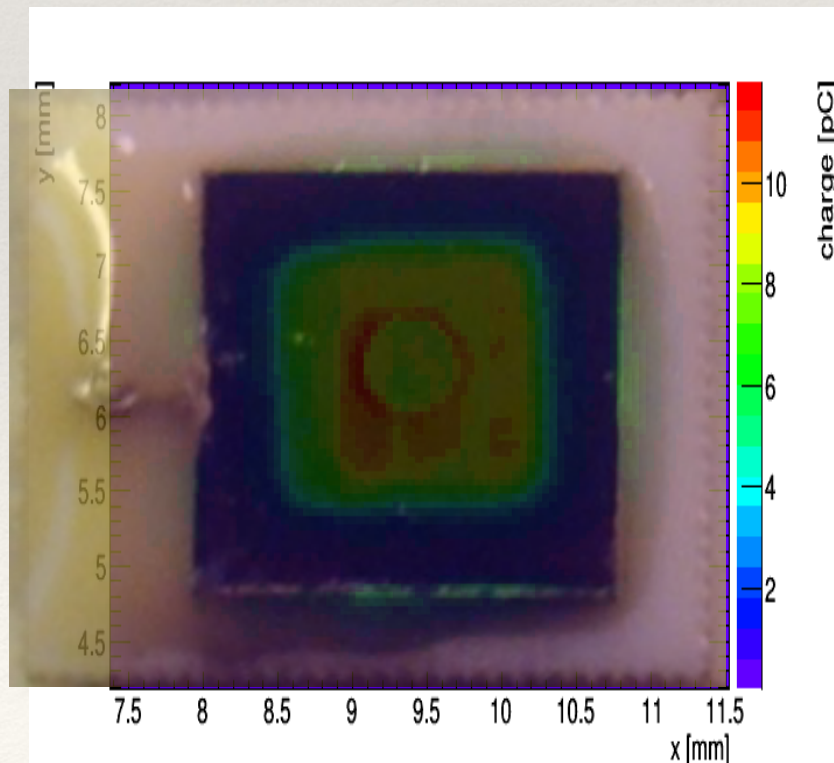
Charge collection outside the active area



IR front @ 1700 V, 20°C

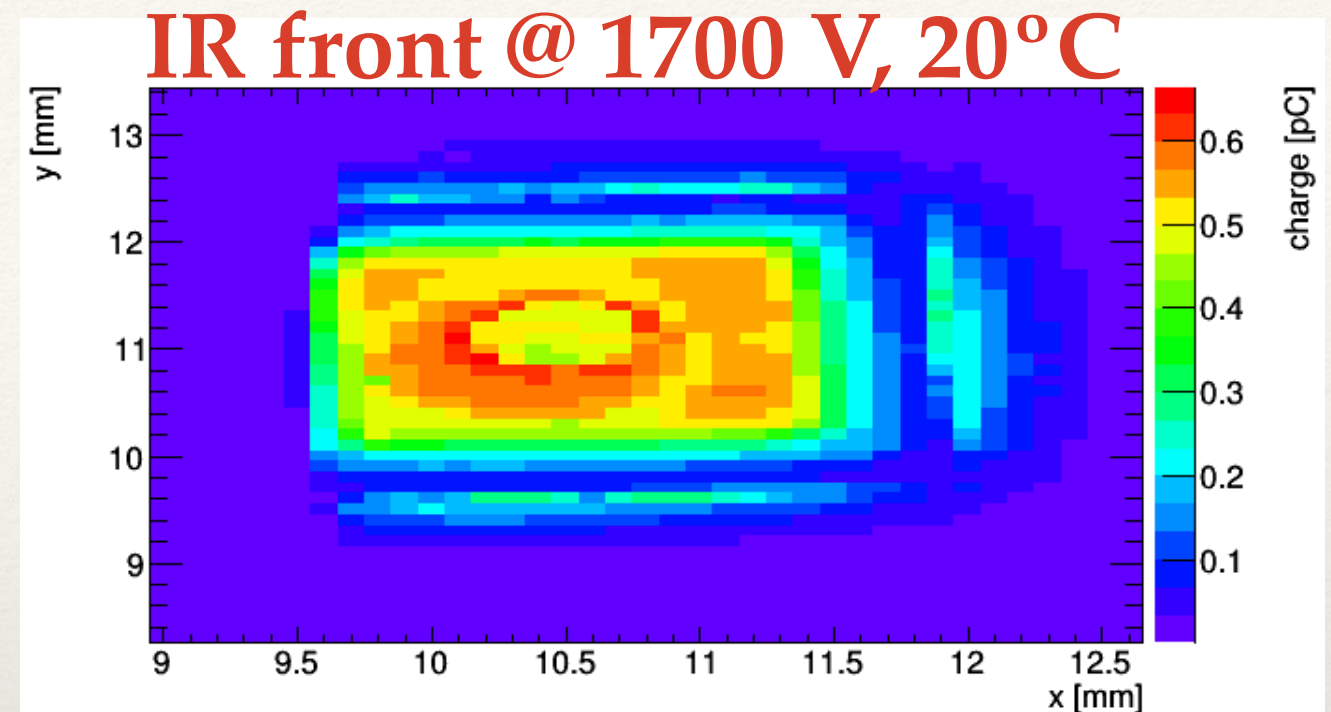


The detector shown here does not belong to the batch characterised in this presentation.

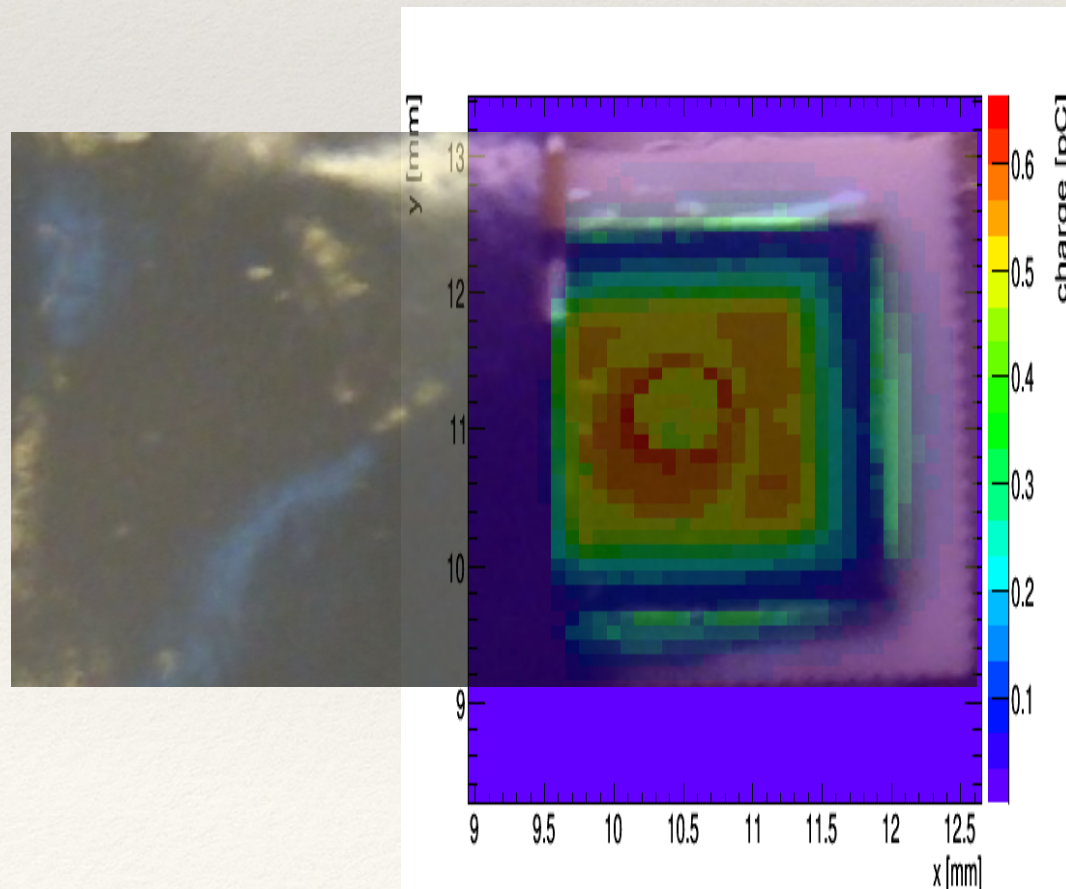


- ❖ The glue surrounding the sensor seems to be causing the laser to reflect and enter the Si even though the laser is not pointed towards it.
- ❖ This would explain the observed charge collection outside the active area of the sensor.

Charge collection outside the active area

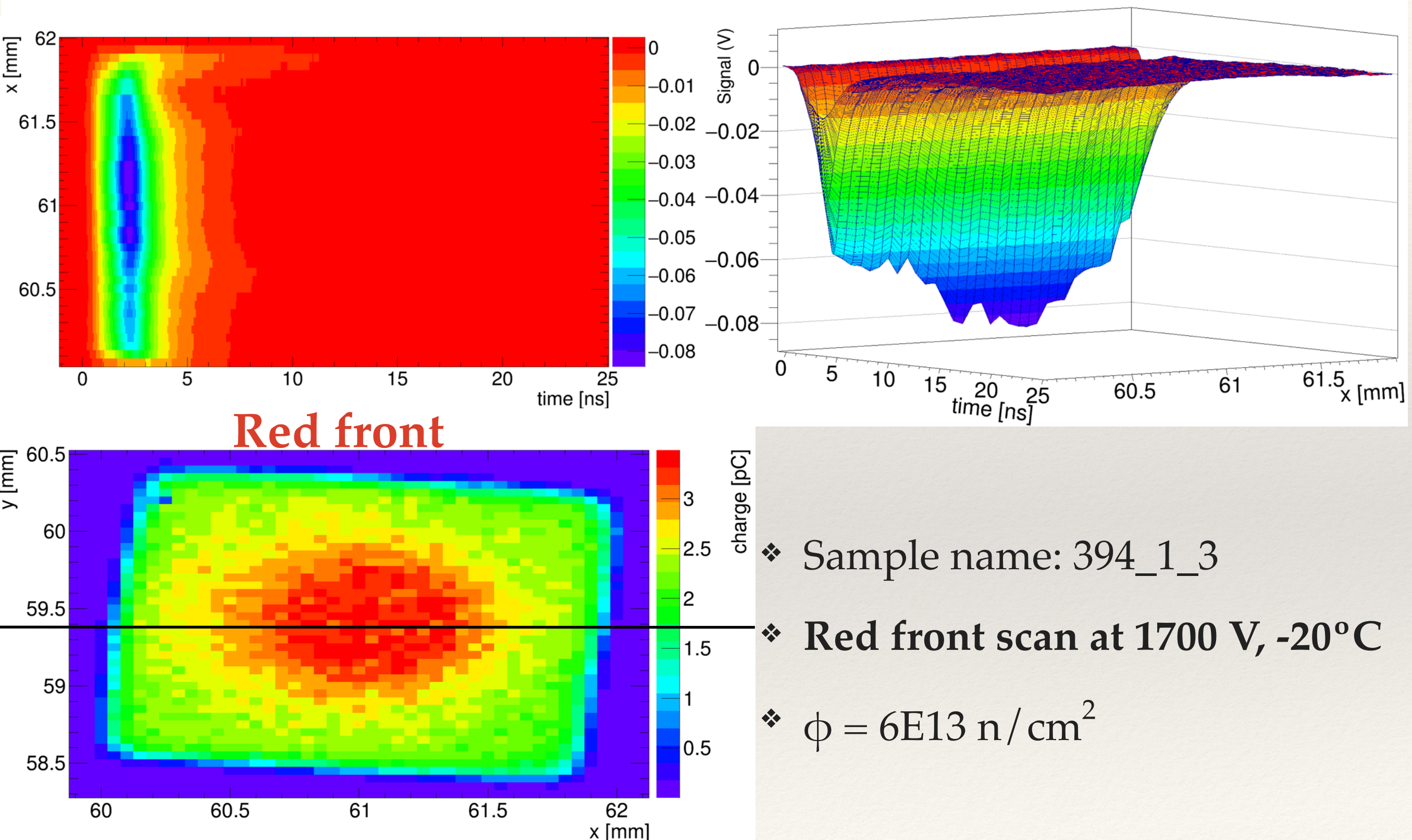


The detector shown here does not belong to the batch characterised in this presentation.



- ❖ We covered one of the sides of the sensor so that a portion of the glue would be concealed.
- ❖ A TCT scan was done and the corresponding odd charge collection area disappeared.
- ❖ We concluded that the abnormal charge collection areas served are due to the reflection the laser on the glue.

Red Scan Inhomogeneity



- ❖ Sample name: 394_1_3
- ❖ Red front scan at 1700 V, -20°C
- ❖ $\phi = 6\text{E}13 \text{ n/cm}^2$